DETERMINING LONG-TERM EROSION RATES IN PANAMA: AN APPLICATION OF ^{10}BE

A Thesis Presented

by

Veronica Sosa-Gonzalez

To

The Faculty of the Graduate College

Of

The University of Vermont

In Partial Fulfillment of the Requirements
For the Degree of Master of Sciences
Specializing in Aquatic Ecology and Watershed Sciences

October, 2012

Accepted by the Faculty of the Graduate College, The University of Vermont, in partial fulfillment of the requirements for the degree of Master of Science, specializing in Aquatic Ecology and Watershed Sciences.

Thesis Examination Committee:

_____ Advisor
Paul R. Bierman, PhD.

_____
Mary C. Watzin, PhD.

_____ Chairperson
Jim O. Vigoreaux, PhD.

_____ Dean, Graduate College
Domenico Grasso, PhD.

Date: May 16, 2012

Abstract

Knowledge of background erosion rates, and the controls on them, is important for evaluating land management practices in Panama, where the proper function of the Panama Canal is linked to water-storage reservoir sedimentation and thus the rate at which sediment leaves the adjacent landscape. This research determined long-term erosion rates in selected watersheds (n=40) in Panama using cosmogenic nuclide analysis. Specifically, I measured ^{10}Be concentration in quartz extracted from river sediments. Sampled watersheds stretch from east to west across the country, and most include at least some of the mountainous spine of the isthmus. This research is the first attempt to quantify erosion rates in Panama at a broad scale.

Landscape physiographic variables, including basin area, relief, and average basin slope, were quantified using a variety of datasets and procedures in ArcGIS. A total of 19 bioclimatic variables, 4 seismicity proxies, surface geology, and a land use proxy were also quantified for each watershed. I assessed the relationship of these variables with erosion rates using bi-variate and multi-variate analysis, as well as ANOVA. I also assessed the grain size effect on ^{10}Be concentrations in stream and landslide samples. Three landslide-related samples were collected and split into seven size fractions to quantify the effect of such rapid sediment inputs on the measured ^{10}Be concentration.

Cosmogenic-inferred erosion rates ranged between 26.1 m/Myr ± 0.6 to 597 ± 62m/Myr. The strongest and most significant relationship in our dataset was found between erosion rate and silicate weathering rate, the mass of material leaving the basin in solution (R^2= 0.726, p= 0.004). None of the physiographic variables showed a significant relationship to erosion (i.e., $p < 0.5$). The number of seismic events in a 10-km buffer is weakly and positively related to erosion rates (R^2= 0.338, p= 0.033); the average magnitude of seismic events in a 100-km buffer (R^2= 0.316, p= 0.047) is weakly and negatively related to erosion rates. This may be indicative that the energy released during seismic events weakens rocks and increases the rate of erosion up to a certain threshold distance. Several bioclimatic variables showed weak but positive relationships with erosion rates including temperature seasonality (R^2= 0.445, p= 0.004) and precipitation during both the driest month (R^2= 0.319, p= 0.045) and the driest quarter (R^2= 0.376, p= 0.017). Two bioclimatic variables showed weak negative relations to erosion rates: isothermality (R^2= 0.381, p= 0.015) and precipitation seasonality (R^2= 0.394, p= 0.012). Tree cover is also negatively related to erosion rates (R^2= 0.351, p= 0.026). Watersheds were clustered into regions according to their location. Spatial analysis at the regional scale strengthened the relationships between variables and erosion rates, but decreased the statistical significance of those relationships. An inverse relationship was found between ^{10}Be concentration and grain size in a set of landslide-related samples. These samples demonstrate both that deep-seated material, which enters streams when such slides happen, carries less ^{10}Be than surface material, and that fine-grained material is preferentially sourced from near the land surface. Due to the small number of grain-size specific samples, no statistical testing can be done to prove differences in isotopic concentration according to their source.

Dedication

I would like to dedicate my work to my dear family. It would have been impossible to achieve this without their support.

A special dedication: in loving memory of my grandfather, Marcelino (Chelo).

Acknowledgements

I want to thank Paul Bierman for his guidance over the past two years. His patience and advice were key in the completion of this research. Special thanks go to Dr. Mary Watzin and Dr. Jim Vigoreaux for their help with my thesis.

I would like to thanks to Dr. Kyle K. Nichols for his help with my data. Thanks to Eric W. Portenga and Lucas J. Reusser for their expertise on ArcGIS and Matlab, that made possible my data analysis. Eric's training in the cosmogenic nuclide laboratory was essential to my research.

Big thanks go to my family and dearest friends for their support during these two years, and for their faith in me. To my office-mates in the Geology Department Grad Office, thanks for sharing the stress and the laughs.

My research was possible thanks to funding from an U.S. Army Research office grant and a Graduate Opportunity Fellowship from the Rubenstein School of the Environment and Natural Resources and the Graduate College of the University of Vermont.

Table of Contents

List of Tables

List of Figures

Chapter 1- Introduction

Quantification of erosion rates, and knowledge of the factors that determine and impact them, are important to many disciplines including aquatic ecology, geomorphology, economics, and natural resources management. Sedimentation of waterways, an effect of accelerated erosion, is associated with deterioration of water quality including increased turbidity and temperature and changes in dissolved oxygen (Bilotta and Brazier, 2008). The yield of water reservoirs can be affected by erosion, because their capacity decreases as they fill with sediment (Harden, 2006).

Ritter et al. (1995) defined sediment generation as the amount of sediment reaching or given access to a channel and sediment yield as the sediment that is discharged from a basin. Erosion rate is defined as the pace at which material is removed from the basin, and is expressed in length by time (Ritter et al, 1995). Denudation and erosion are often used interchangeably; however, denudation accounts for the sum of the overall erosive process over a long term (Summerfield, 1991). Erosion accounts for the mechanical erosive processes that remove solid material, while denudation also considers chemical weathering that results in a dissolved load. For the purpose of this work, sediment generation and erosion rates will be used interchangeably; that is assuming no change in storage, or stated otherwise, equilibrium between the rate at which sediment is generated and the rate at which it is removed from the drainage basin over millennia.

Erosion has been quantified using both proxies and direct measurements. Suspended sediments have been measured to estimate contemporary erosion rates (see

Judson, 1968). Dams and reservoirs have been used to determine erosion rates by measuring water level at two given times, and attributing the change in water volume to sedimentation (Stroosnijder, 2005). Cosmogenic nuclides emerged as a proxy for erosion rates in the mid 1990s (Bierman, 1994). This method can be used in a variety of landscapes. However, cosmogenic isotopes have been scarcely applied in tropical climates (Portenga and Bierman, 2011). This research will use cosmogenic nuclides as a method to constrain background erosion rates in the tropics of Panama.

Erosion rates are influenced by natural factors such as geology, slope, and climate but can increase dramatically due to human activities (Douglas, 1969; Ouyang et. al, 2010) such as deforestation and the creation of impervious surfaces (Foley et al., 2005; Marshall and Shortle, 2005). Erosion rates are thought to be higher in tropical environments than in template and dry climates (Douglas, 1969; El-Swaify et al., 1982; Lal, 2000).

Objectives

My research aims to determine long-term, background erosion rates in Panama (Figure 1.1) using ^{10}Be measured in quartz extracted from river sediments. It is important to know background erosion rates in order to make land management decisions in the context of natural process rates. Even though a considerable number of studies use ^{10}Be as a proxy for erosion rates, just a few of them are in tropical environments (tropical river sediment samples number 98 of 1599 total of which 17 of the 98 are from Panama; Portenga and Bierman, 2011).

Obtaining erosion rates for 40 watersheds in Panama (Figure 1.2) allows me to place human impact in the context of background erosion rates and gain knowledge about the relationship of erosion rates, in a tropical climate, to physiography, tectonic activity, geology, and biologic features. This research will expand the breadth of environments where cosmogenic isotopes have been measured and provide important information for the management of the Panama Canal, in particular, the lifetime of the reservoirs integral to canal operation.

The effect of physiographic controls on erosion and sediment movement has been long debated. Watershed elevation appears to exert control on erosion at a global (Portenga and Bierman, 2011) and at a site-specific (Palumbo et al., 2009) scale. Portenga and Bierman (2011) found that mean basin slope significantly relates to drainage basin erosion rates at both local and global scale, and that relief is important in controlling erosion rates in the tropical climate zones. However, von Blanckenburg (2004) concluded that relief alone does not lead to accelerated erosion. My research aims to shed some light on these physiographic controls on erosion in tropical climates.

My sample set allows me to investigate the importance of sediment delivery to rivers by discrete landslide events. Brown and others (1995; 1998) related ^{10}Be to sediment delivery processes by doing grain-size specific ^{10}Be analysis. Fine material located at the surface has been exposed to cosmic radiation longer than coarser material (sourced at depth) and thus has higher isotopic concentrations. Measuring ^{10}Be in a variety of size fractions allows me to quantitatively determine the impact (on ^{10}Be

concentration) of sediment input due to landslides. Sediments samples were taken at the intersection of a recent landslide with the river, as well as up and downstream from it. This research will explore mass wasting-dominated sediment delivery in the watershed from which landslide samples were obtained.

Study Area

Location

Panama is the southernmost Central American country. It is located between latitudes 7° 12' 07" and 9° 38' 46" and longitudes 77° 09' 24" and 83° 03' 07". The country comprises an area of 75,517 km^2 (Contraloría General de la República de Panamá, 2008). It is limited on the north by the Caribbean Sea, on the south by the Pacific Ocean; on the east it shares borders with Colombia and on the west with Costa Rica (CGRP, 2008).

Climate

Panama's climate is tropical; more specifically, its climate is defined as tropical maritime with influences from the Caribbean Sea and Pacific Ocean (Contraloría General de la República de Panamá-Instituto Nacional Estadística y Censo, 2005). The climate is characterized by high year-round temperatures, with low diurnal and annual range, abundant precipitation, and high relative air humidity.

Generally, there are two seasons: a wet and a dry one. The wet season goes from May to December, and the dry one from December to April (CGRP-INEC, 2005).

However, there are some differences between the Caribbean and Pacific slopes. The Pacific's side mean annual precipitation ranges from 1,500 to 3,500 mm, and the difference between the wet and dry seasons is marked. On the Caribbean slope, precipitation is more uniform year round, and no marked difference exists between the seasons. Precipitation there exceeds 4,000 mm annually.

Temperatures are high year round. Annual mean temperatures range between 24°C and 28°C; the average diurnal temperature range is approximately 1.9°C on the Caribbean slope and ranges between 1.5 and 2.5°C on the Pacific side (CGRP-INEC, 2005).

Geography

Panama is mostly flat, with a Central Cordillera extending along most of the isthmus from the border with Costa Rica to the Panama Canal (Palka, 2005). This Cordillera has several regional names; it is called Cordillera de Talamanca in Costa Rica, Serranía de Tabasará as it crosses into Panamá, and Sierra de Veraguns as it approaches the Canal Zone (Palka, 2005).

Panama's maximum elevations are located in the southwestern province of Chiriquí: Barú volcano (3,475m) and Cerro Picacho (2,986m) and the northwestern province of Bocas del Toro: Cerro Fábrega (3,335m), Cerro Itamut (3,279m) and Cerro Echandi (3,162m) (CGRP-INEC, 2005). San Blás Islands, composed of about 350 islands, lie on the Caribbean coast of Panama; there are over 1,000 islands on the Pacific Coast (Palka, 2005).

There are eighteen major watersheds draining into the Caribbean Sea. These rivers average 56km in length, have an average slope of 5.5%, and discharge greater volume than the Pacific ones, due to their short distance from the mountains to the sea, and high precipitation (CGRP-INEC, 2005). The major rivers in this region are the Chagres (125 km long), Changuinola (118 km), Indio (97 km), Circamola (83 km) and Sixaola-Yorkín (70 km) (CGRP-INEC, 2005).

Thirty-three major rivers drain into the Pacific Ocean. These rivers are longer than those draining to the Atlantic, averaging 106 km, and have lower slopes, with an average of 2.27% (DEC, 2005. The major rivers are the Chucunaque (231 km long), Tuira (230 km), Bayano (206 km), Santa María (173 km), Balsas (152 km), Chiriquí Viejo (128 km), La Villa (119 km), Tabasará (109 km) and Grande (97 km) (CGRP-INEC, 2005).

Geology

The first detailed texts on the geology of Panama were published by Schuchert (1935) and Terry (1956). This section provides an overview of Panama's geology based on their work and publications.

Panama is mostly composed of volcanic rocks. The Canal Zone is mostly composed of volcanic tuffs from the Miocene era. These can also be found in the eastern region of Darien. The geology of eastern Panama consists mostly of volcanic tuffs and ashes, with small limestone areas. There are regions on the east where limestone is found with dark clay shale formations and sands. A region of tuffs, ash and lava blended with

marine and terrestrial sediments extends west from the central Canal Zone. To the west, by the province of Bocas del Toro, the sedimentary column is made of a limestone-volcanic series of Eocene age. It also includes conglomerates, sandstones, shales and sandy limestones of Miocene age.

Metamorphic rocks are rare in Panama. Schist has been reported on the eastern province of Darien. Small slate outcrops have been reported in several provinces stretching from the center to the west, close to the Costa Rica border. Sedimentary rocks are mostly limited to the eastern region of Panama with a few exceptions on the west.

The basement complex, underlying surficial rocks, is mostly composed of extrusive volcanic, flows, agglomerates and tuffs that have little metamorphism but much deformation. The sedimentary rocks are mixed with the lavas not older than Cretaceous.

A more recent work on the geology of Panama was published by Escalante (1990). The following information is generalized from Escalante's work. An overview of the Canal Basin profile, starting on the uppermost strata is as follows: Late Miocene fine grained sandstone and siltstone, followed by Middle Miocene tuffs and calcareous, as well as sandstone and conglomerate. Clays, shale, mudstone, siltstone, conglomerate and limestone, all from the Early Miocene, can also be found. Generally, the last three sections are dominated by volcanic materials, conglomerates and siltstones all the way down to an undivided deeply weathered volcanic rock basement.

The Tuira-Chucunaque Basin formation on the east of Panama is composed of sand, gravel and silt on its uppermost strata. Shale and sandstones dominate the lithology, and, to a lesser extent, limestones. The basement is made up of mafic igneous rocks.

The dominant bedrock geology in the watersheds included in my research is tertiary volcanic rocks, present in 33 of the 40 watersheds. Only three watersheds have sedimentary rocks and four have igneous intrusive rocks as their main geology type.

Tectonic setting

The geological development of Panama is fairly recent and it can be understood in the plate tectonic paradigm (Harmon, 2005). The isthmus where Panama is located is the result of a collision of the Panama-Choco island arc with South America. This took place in the late Miocene-Pliocene (3.5-7 million years ago).

Adamek and others (1988) were the first ones to suggest the existence of a microplate they called the Panama-Costa Rica microplate. This microplate also includes most of Costa Rica, and is also referred to as the Panama Block. It shares borders with the Caribbean plate on the north, Cocos plate on the southwest, Nazaca plate to the south, and the South American plate to the east and southeast (Camacho et al, 1997) (Figure 1.3).

Kellogg and Vega (1995) combined Global Positioning System measurements, geologic, gravity and seismic data to derive a tectonic model of the North Andes and Southern Central America region. They concluded that the Panama-Costa Rica

microplate is moving northward relative to the Caribbean plate, and that it continues to collide eastward with the northern Andes.

Camacho and others (1997) conducted a seismic hazard assessment for Panama. Their work resulted, among other findings, in the production of peak ground acceleration maps for Panama's main cities. They found that the highest hazard is on the western side of the country, close to the Panama Fracture Zone (Figure 1.3) and the western segment of the North Panama Deformed Belt and to the southeast of the country close to the Panama Block-South America plate margin. All these geologic features play a role in seismic events. The lowest seismic hazard was found in Central Panama. The Pacific side is characterized by its geologic activity, having a deep oceanic trench, narrow marine shelf, and active subduction (responsible for volcanic activity and earthquakes). On the other hand, the Atlantic side is a passive, stable margin with a broad marine shelf (Harmon, 2005).

Forested land cover

Panama's forest resources are divided in three categories: production, protection, and special (ANAM, 2004). In 1950, forest was estimated to cover 70% of the country's territory but only 40.4% by 1998 (ANAM, 2004). Forest cover was estimated to be 45% for 2000; as of 2003, only 44.4% of Panama's territory was forested (Ramírez, 2003). According to a report published by the Autoridad Nacional del Ambiente (ANAM) in 2004, mature forests represent the greatest percent of forested land use. Most of the

forests are located in the Atlantic slopes, since human activity has historically been more intense on the Pacific side (ANAM, 2004).

Currently, agriculture is the main driver of deforestation in Panama (ANAM, 2004). Slash and burn, conversion to grasslands, and monoculture plantations are the main reasons behind deforestation. Other reasons leading to deforestation are associated with timber harvesting, mining activities, and urban development (ANAM, 2004).

Both the south central province of Los Santos and the western province of Chiriqui, have seen the greatest recovery in forested area, as shown in reports from Panama's government reports. These reports have also shown that the provinces where agriculture is taking over the forests at a rapid rate are: Darién, Eastern Panama, Bocas del Toro, Coclé, Colón and the trans-isthmus region (ANAM, 1993; ANAM, 2003) (Figure 1.4). On the other hand, the establishment of protected forested areas has increased in Panama. In 2000, protected areas accounted for 26% of the land; by 2008, protected land increased to 36% (Haruna, 2010).

Thesis structure

In chapter 2, I review some of the available scientific literature related to methods for determining erosion rates, interpreting cosmogenic nuclides, and understanding the effects of sediments on aquatic biota. Chapter 3 contains a detailed methodology of the procedures used in my research. In chapter 4, I present my data and in chapter 5, I discuss those data. Finally, chapter 6 includes my conclusions and suggestions for future work.

Figure 1.1 Panama location. Panama is delineated by the broader outline. Map data from ESRI.

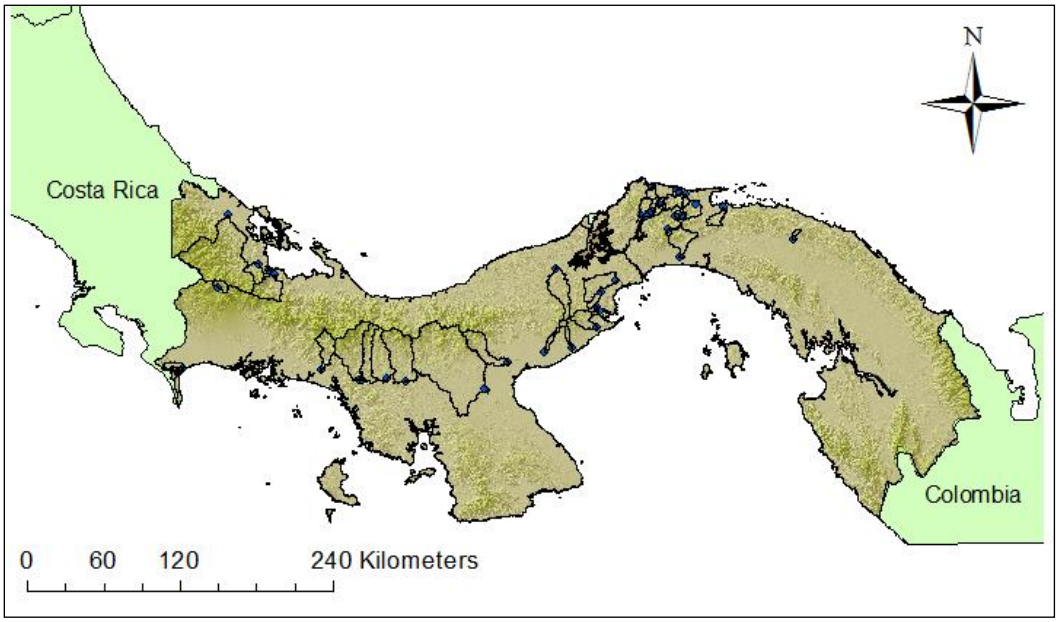

Figure 1.2 Sampled watersheds, country of Panama, shaded relief map. Sampling locations are indicated with blue dots, and the watersheds draining to them have been delineated and are outlined. Map data from CGIAR-CSI.

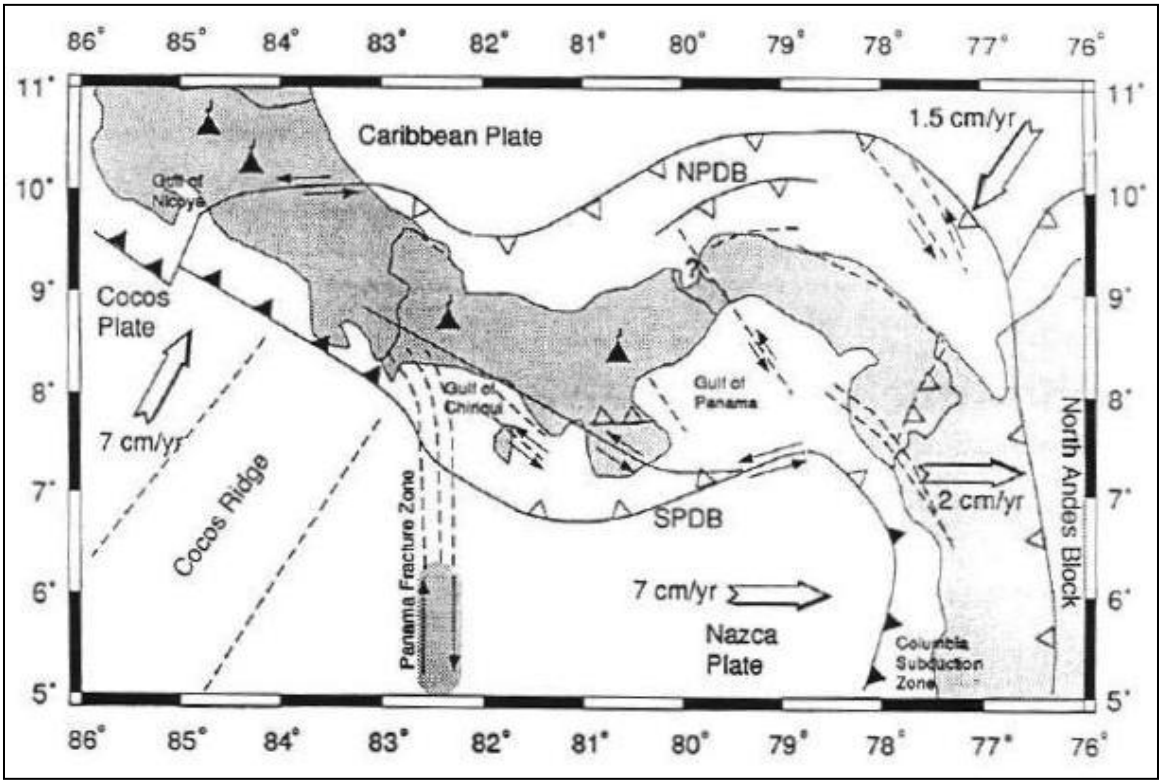

Figure 1.3 Tectonic features in Panama. Figured published by Camacho et al., 1997

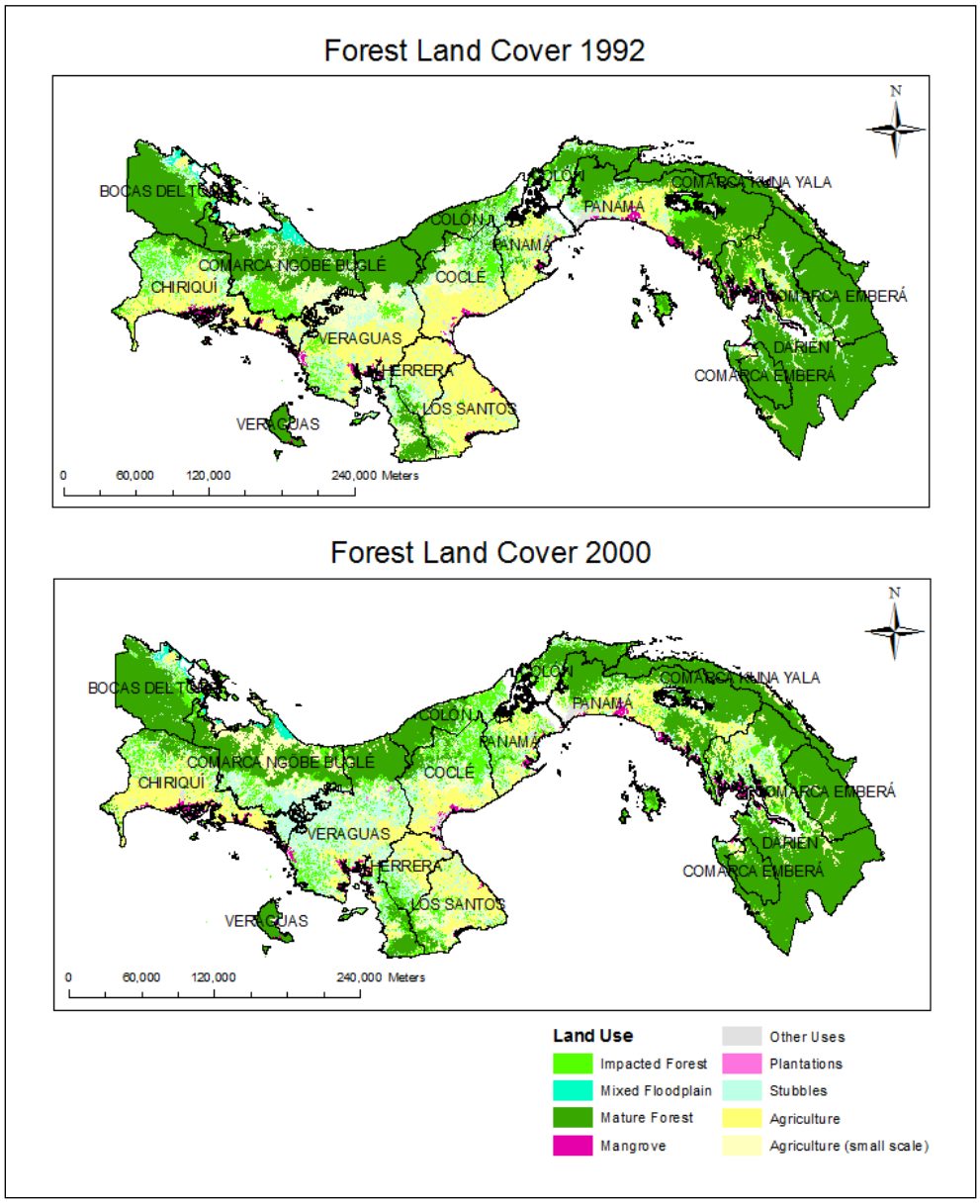

Figure 1.4 Forested land in Panama. Forested land use change by province (1992-2000). Map data downloaded from the Smithsonian Tropical Research Institute GIS Data Portal.

Chapter 2- Literature Review

Human impacts on the environment and natural resources

Human impacts on the environment and natural resources have motivated research for the last century (Marsh, 1864). Humans have been considered as geomorphic agents (Hooke, 1994; Hooke, 2000), sculpting the landscape as it fits our needs and desires. In some cases, human activities are greater than the sum of all natural processes operating on earth surfaces by as much as an order of magnitude (Wilkinson, 2005). Although erosion rates, and thus rates of sediment supply to watersheds, are related to natural factors, such as geology and climate, accelerated erosion is often triggered by human activities (Douglas, 1969; Ouyang et al., 2010). In a study in the Ecuadorian Andes, Vanacker et al. (2007) concluded that removal of vegetation cover in that area increased sediment fluxes exponentially by a factor as high as 100.

The effects of land use and land cover changes, driven by human settlement and economic activities include increases in the rate of soil erosion, sedimentation, turbidity, as well as modification of streamflow regimes and aquatic habitat alteration (Bullard, 1966; Wilkinson, 2005). Land use changes, including forest cover decrease, agricultural practices, grazing, urbanization and road construction, affect the amount and timing of runoff and sediment transport. Deforestation and land clearing, as well as conversion of land to agriculture have been the main drivers of landscape change and have increased the frequency of natural processes such as landsliding. Deforestation can be related to urban sprawl, timber harvesting, and mining, among many other uses. An increase in

construction and bare land increases erosion and sediment load (Wolman, 1967; Wolman and Schick, 1967; Foley et al., 2005; Ouyang et al., 2010).

Water quality issues

Access to clean water and the ability to grow food controls societies' ability to survive and develop. Both the soil capacity to grow crops and the quality of water are affected by soil erosion. Sediment resulting from erosion affects water both physically and chemically.

Deforestation, development, agriculture, and the increase of impervious surfaces in watersheds can significantly increase erosion and sediment loading to streams and rivers (Foley et al., 2005; Marshall & Shortle, 2005). Removing forest coverage reduces the amount of rain that is intercepted before it reaches the surface, causing an increase in material that is subject to sheet erosion (Sidle et al., 2006). Deforestation increases the amount of raindrop erosion, since nothing reduces the force of the water before it hits the surface. Reduced evapotranspiration, therefore increased water saturation in the soil, is an effect of forest removal (Díaz et al., 2007)

Sediments result in an impairment of water resources, limiting their use (USEPA, 2000; Chao et al., 2007). Increased turbidity due to suspended material reduces the aesthetic value of a water body (i.e. river, stream, and coastal waters), which in turn can decrease its attractiveness for swimming and fishing activities. However, the effects of sediments are not limited to human health and water use; there are serious consequences to aquatic life. High turbidity increases the percentage of incoming solar radiation that is

reflected off the water, decreasing the water temperature (Ryan, 1991). This can have a deleterious effect on temperature-sensitive species populations. Many contaminants have a high affinity with solid matter (Massoudieh et al., 2010), so they reach water bodies adsorbed onto sediments. Heavy metals, bacteria, and organic matter introduced in sediments can trigger chemical changes in streams. Sediment-associated organic matter can lower dissolved oxygen levels (Bilotta and Brazier, 2008). Physical habitat for aquatic species can also be altered with an increased sediment transport.

Aquatic biota depend on certain habitat characteristics for their survival and reproduction. Such characteristics include specific water depth, water velocity, flow amount and variability, substrate, extent of pools versus riffles, vegetation and the existence of undercut banks (Soulsby et al., 2001; Diana et al., 2006). These conditions are altered by sedimentation and erosion. As concluded by Wilber and Clarke (2001), sediment deposition and settling in gravel-bed rivers decreases development and survival of fish eggs. An increase in fine sediment in gravel spawning beds can suffocate fish embryos (Randhir and Hawes, 2009), eventually reducing the adult population that is able to reproduce. Deposited material can block the pores on the gravel-redd structure, altering the exchange of dissolved oxygen with the water (Bilotta and Brazier, 2008). An increase in silt and clay in the water column can result in clogging of gills in fish and mussels, reducing filtering and respiration (Randhir and Hawes, 2009). Erosion of the river banks can reduce spawning habitats.

Macroinvertebrates can be affected by suspended sediment that attach to periphyton and reduce their attractiveness for grazing (Bilotta and Brazier, 2008). The main effect on macroinvertebrates is the reduction of habitat due to sediment deposition. An indirect effect of sediments on fish populations is the reduction in net primary production. Sediment suspension in the water column reduces light penetration, which in turn reduces phytoplankton and other primary producers' activity (Matson et al., 1997). This reduction will decrease food sources for both invertebrates and fish.

Sediment sourcing to waterways

Sediment is sourced from erosion at both the watershed scale and from channel banks (Trimble, 1997). There are several ways by which sediment reaches streams: soil creep, overland flow, channel and bank erosion, and mass wasting (Bierman and Nichols, 2004; Randhir and Hawes, 2009).

Sediment derived from watersheds that had some construction activities increased by 2 to 200-fold as compared to rural settings, and mostly wooded watersheds (Wolman and Schick, 1967). Forested watersheds, as well as those having only riparian forests, act as sediment traps (Norton and Fisher, 2000). In a study comparing the impact of vegetative cover types under different land uses in Palestine, Mohammad and Adam (2010) found that deforestation is the only land use that surpasses cultivated areas in terms of soil loss. That same study concluded that deforestation is directly related to an increase in runoff and soil erosion. In a study looking at deforestation and its consequences in an Ecuadorian Andes watershed, Vanacker et al. (2007) concluded that

areas with high vegetation cover erode at rates similar to natural ones, regardless of vegetation type.

A review of the effect of land uses on soil erosion in Mediterranean ecosystems in Spain stated that without exception, deforestation and substitution of forests by croplands leads to a dramatic increase in soil erosion (García-Ruiz, 2010). Harden (2006) studied human impacts on headwater fluvial systems in the Andean region, and found that forest clearing for cultivation increases sediment yields by 2 to 3 orders of magnitude. The relationship between deforestation, erosion and sediments holds in varied climatic regimes, indicating that this is an environmental concern on a global scale. The benefits of forest cover are lost with deforestation; as sediment load to streams increases.

Agricultural lands have the highest sediment yield of all land uses (Pimentel et al., 1995; Foley et al, 2005; Wilkinson, 2005; Montgomery, 2007). The relationship between erosion and agriculture is complex; not only do agricultural practices increase soil erosion and sediment loading, but erosion reduces soil fertility and degrades the land, fostering new deforestation events as infertile land is abandoned and new agricultural settlements are founded.

In a study in Ohio, Tong and Chen (2002) concluded that in watersheds where agricultural and/or urban land uses were dominant, the amount of sediment delivered to streams increased, especially after rain storms. Reviewing the impacts of humans on erosion and sedimentation, Wilkinson and McElory (2007) estimated the global mean soil lost as a consequence of agricultural activities to be ~600 m/my (0.06mm/yr) in areas

under cultivation. Their conclusion echoed many other researches on the direct relationship between agricultural practices and erosion.

Not only does the conversion of forest to agriculture trigger soil erosion, but the intensification of agricultural practices makes the situation worse. Intensification of agriculture has effects that range from local to global in scale. Locally, increased soil erosion, decreased soil fertility, and reduced biodiversity are common. On a regional scale, groundwater pollution, eutrophication of rivers and lakes can take place. Atmospheric constituents of climate can be altered, as a global-scale consequence (Matson et al., 1997). Water and surface radiation balances can change due to forest clearing (Foley et al., 2005). Conversion of forests to agriculture adds CO_2 to the atmosphere, because carbon sequestration services from trees are lost (Dixon et al., 1994; Vitousek, Mooney et al., 1997).

Not only must one consider human-induced increase in erosion, and their effects on water quality and aquatic life, but it is important to consider sediment sinks. Erosion takes place almost entirely in catchment headwaters (Wilkinson, 2005) and sediment makes its way to low-lying areas and water systems, as a result of different transportation mechanisms. Sediments accumulate behind dams in reservoirs reducing their lifetime (Christiansson, 1979; Matson et al., 1997; Syvitski, 2005; Harden, 2006). Ubolratana dam's (Thailand) capacity has been reduced by 1.4% in a 25 year period (1965-1990) due to sediment deposition (Sthiannopkao et al., 2007). The Paute hydroelectric project, in Ecuador, is also threatened by severe erosion that is likely to reduce its life span

(Vanacker et al., 2003). The vast majority of material eroded from a watershed is stored close to its source, including river beds and banks, and only a small amount makes it way out of the basin (Trimble, 1977; Wilkinson and McElroy (2007).

Erosion rate quantification with indirect measurements

Scientists have used a variety of methods to quantify erosion. These include mathematical modeling, isotopic and sediment loading measurements, and varied field methodologies. Recently, remote sensing has been used to study erosion.

Sediment yields coming out of watersheds have been used as a proxy to infer contemporary erosion rates. Menard (1961) studied present and past regional erosion rates in the Appalachian, Mississippi, and Himalayan regions under the assumption that present-day erosion rates can be estimated from the sediment load transported by rivers. Average past regional rates of erosion for a particular time interval can be determined if the source region area, volume of sediments deposited, and timeframe of the erosion are known. Bed and suspended loads were used in combination with area information derived from geologic maps, and sediment accumulation estimates (offshore) using seismic observations. Duration of erosion was broadly approximated to geologic periods. Both contemporary and long-term erosion rates were determined and compared in Menard's research. He concluded that the Mississippi region has been eroding at the same rate for the past million years; the Appalachian region was eroding slower than in the past million years, and the Himalaya region was eroding faster than in the past million years.

Contemporary erosion rates have been estimated using rivers' suspended load data. In 1968, Judson measured material carried by streams at the point where they exit drainage basins, as a method to integrate erosion rates over larger areas but shorter time scales. As an alternative to measuring the mass flux in streams, he suggested the quantification of material deposited in a reservoir or lake for a specific time would be indicative of the rate at which the land eroded in the basin upstream from the standing water. Dividing the volume of sediment by the basin area gives the erosion rate of the basin. Judson noted that the erosion rate is not uniform throughout the basin. He pointed out that measuring the amount of suspended material that passed through a gauging station was also a way to quantify erosion rates, and that doing so along several sections of a river, varying in the area upstream contributing waters to it, would show that sediment yields vary over a watershed. According to Stroosnijder (2005), dams and reservoirs at the outlet of a watershed can be used to determine erosion rates by way of measuring storage changes. Measuring the water depth in the reservoir at two given times, and attributing the change in storage to sedimentation, would give an estimate of the sediment that has accumulated in the reservoir over the time period between level measurements.

In his work aiming to quantify the relationship between denudation and geomorphology, Anhert (1970) justified the use of sediment transport of streams as a means to determine denudation rates, with a realization of the pitfalls of direct denudation measurements. Erosion processes are sensitive to environmental change, and the instrumentation installed to measure denudation on the slopes could interfere with the

process. Anhert stated that the determination of denudation using sediment yields was the best method to date, although recognizing that the method assumed equilibrium - between sediment production, transport, and the rate at which it exits the basin during the short period of time considered in suspended load sediment records. Transported sediment was measured in streams, assuming that they carried material from the watershed above, and that all material would pass through that section of the river. Knowing the mass of transported sediments, mean area draining to that section of the river, and mean density of the rock material, he determined mean basin denudation rates.

Trimble (1977) estimated upland erosion using soil profile truncation in the Piedmont region of the United States. He measured depths of soil loss in the field, and paired them with degrees of soil erosion as previously published on erosion surveys. Trimble concluded that most of the eroded sediment was stored in the watershed, and only 6% is exported, and that sediment transport is impeded by reservoirs.

Costa (1975) quantified surficial deposits in the Piedmont province of eastern North America, by way of soil profile thickness, and reservoir sedimentation to estimate the percentage of sediment leaving the system. He also quantified the sediments deposited in floodplains to measure the storage and retention in the system. Radiocarbon dating was used in wood fragments found in alluvial deposits to constrain the time since the deposition. His work was based on the assumption that the volume eroded from a watershed equaled the sum of the sediment transported through the system and out of it, plus the volume of sediment stored within the watershed. Costa stated that 34% of eroded

material (since 1700s) has been exported from the system, as inferred from reservoir sedimentation. Some of the sediment, 14%, remains as alluvium material in the upper 1m of flood plains. The remaining material, 52%, is stored in colluvial-sheetwash deposits in hillslopes.

Dedkov and Moszherin (1992) synthesized suspended sediment yield data from mountain regions worldwide as a way to characterize erosion and assess the intensity of erosion due to natural and anthropogenic factors. These researchers recognized that sediment yield is not an accurate measure of erosion and mechanical denudation because eroded sediment is stored within the basin. However, they acknowledge that sediment yield can be used to compare erosion intensity under different conditions (both natural and human-induced) because sediment yield depends on erosion and mechanical denudation. In the basins, data on area, relief, runoff, geology, landscape patterns and extent of human impact on the landscape was collected to compare to the sediment yields. They concluded that intense erosion was due to high precipitation amounts and intensities, high runoff, mountain relief, intense recent tectonic activity, and conversion to agricultural lands.

In a study of soil erosion and control practices in the Palouse River Basin, WA, Ebbert and Roe (1998) measured suspended sediments as a proxy of erosion. Long-term annual yield data from USGS monitoring stations was compared to estimates of soil erosion derived from field measurements in agricultural plots. They concluded that the

correlation between those datasets provided a reasonable estimate of erosion rates in the watershed.

In order to quantify erosion associated with discrete events in the Caspar Creek Watersheds, CA, Lewis, (1998) used data from an inventory of slope failures greater than $7.6m^3$. The database was updated once a year, minimum. The volume of displaced material was obtained with tape measurements on landslide scars. In order to estimate erosion at a broader scale, erosion plots were located in each of the sub-watersheds included in the study. Sediment loads were compared between the North and South Fork gaging stations to look at the effect of logging and other land management practices. This research concluded that suspended loads increased by as much as 212% following logging activities.

Erosion rate quantification with direct measurements

Erosion can be measured directly by way of change in weight, surface elevation, channel cross section, and sediment collection from erosion plots and watersheds (Stroosnijder, 2005). Stroosnijder distinguished the adequate scale for each method as follows. Local mass transport can be quantified by change in weight in areas of a $1m^2$. The method consists of splash cups to collect material, detached from the soil as a result of erosion. For studies including areas under $100m^2$, sediment collectors are located at the lower end of a plot to collect sediments that moved downslope and thus quantify erosion. Areas $500m^2$ or less can be measured using erosion pins; according to the author, erosion pins are particularly useful for monitoring hillslope erosion. The method consists of pins

inserted in the ground and used to measure the distance to the soil. An increase in such distance implies hillslope denudation (erosion), whereas a decrease implies material accumulation (sedimentation). Sirvent and others (1997) used erosion pins to determine the rate of ground lowering. Readings of the pins took place every six months and the record was analyzed to generate ground lowering contour lines. Measuring changes in cross sections is an ideal means by which to quantify channel erosion: cross sections of a river are measured at a known time interval, and the difference is used to estimate the volume of sediments that has been lost to erosion. Flumes are useful at the watershed scale, because they measure the water height (which in turn is used to estimate water volume) and one can take samples to quantify suspended sediment concentration. Which, when convolved with discharge provides an estimate of sediment transport.

Remote sensing and geographical information systems

More recently, remote sensing has been used in erosion-related research. Satellite data and aerial photo interpretation can be applied to detect both erosion and its consequences (Vrieling, 2006). One of the benefits of using remote sensing as a proxy for erosion rates is that successive images can be used to identify change over time including sediment sources. Development of features indicative of landscape-sculpting processes, for example landslides and gullies- can be tracked using remote sensing and related to sediment load increases in streams. Low resolution imagery (15 m scale or greater) can be used for regional studies, comprising areas greater than 10,000ha; high resolution imagery (meter-scale) is useful in areas under 10,000ha (Stroosnjider, 2005). Remote

sensing is also useful for building erosion models, because it helps quantify landscape variables, like land cover changes, over a given timeframe, like land cover changes (Stroosnjider, 2005). This provides options and flexibility to use remote sensing and aerial imagery as tools when measuring erosion.

Doing research in St. John (United States Virgin Islands), Ramos-Scharrón and MacDonald (2007) measured sediment production on the field, and used that information to validate a GIS-based model for erosion intensity. Streambank erosion was measured using erosion pins for 2 years and converted to sediment yield using source bulk density. Sediment fences were used below undisturbed hillslopes. These fences are built with geotextile silt fence fabric, and used to measure hillslope erosion directly. They are located in the slopes to collect eroded material, the volume of which is quantified and analyzed (Rochibaud, 2005). An ArcInfo based program (STJ-EROS) was developed to calculate sediment yield, from a variety of sources, at a watershed scale. The aim of this was to quantify the amount of sediment reaching marine environment. Sediment yields predicted by the model were similar to those measured in the field.

Thoma and others (2005) used airborne laser data (LiDAR) to assess riverbank erosion in Blue Earth River, MN. Images obtained a year apart were corrected for the vegetation returns. After correction and comparison of the images, the resulting surfaces files only differed in their elevation (z value from x,y,z, coordinates). The summed differences were divided by the spatial extent of the digital images to obtain a net volume

change due to erosion or deposition in the year that passed between scans. Multiplying average bulk density by the estimated volume change yielded mass loss estimates.

Cosmogenic nuclides as a proxy for erosion

During the 1990s, cosmogenic isotopes emerged as the premier method to estimate long-term or background erosion rates from sediment (Bierman, 1994; Bierman and Steig, 1996; Brown et al., 1995; Granger et al., 1996). Cosmogenic nuclides provide a robust method to quantify erosion rates, because they integrate enough time to average out extreme events on decadal and centennial time scales. These isotopes have the potential to provide long-term data that can help place human influences on the landscape and its processes, in context (Bierman and Nichols, 2004; von Blanckenburg, 2005).

Isotopic production

Cosmogenic isotopes are formed when earth materials are exposed to cosmic rays (Lal and Peters, 1967). ^{10}Be is produced by spallation reactions in quartz. A spallation reaction is a high-energy process, during which a neutron collides with a target nucleus and breaks it into several particles, resulting in a lighter residual nucleus (Gosse and Phillips, 2001) and the emission of neutrons and protons. As a result of this interaction, a variety of otherwise rare isotopes (such as ^{3}He, ^{10}Be, ^{21}Ne, ^{26}Al, and ^{36}Cl) accumulates in rock and soil and are called *in-situ produced cosmogenic nuclides*. These isotopes are also formed in the atmosphere, due to similar reactions, and the non-gaseous isotopes (^{10}Be, ^{26}Al, and ^{36}Cl) are delivered with precipitation (Gosse and Phillips, 2001).

Quartz is the ideal mineral for the analysis of ^{10}Be, due to its crystal structure. This structure prevents contamination with meteoric ^{10}Be (that is formed in the atmosphere), and its mechanical stability makes it resistant to weathering and easy to isolate from other minerals, as well as any meteoric ^{10}Be, by way of acid etching (Lal and Arnold, 1985; Gosse and Phillips, 2001;Tuniz et al., 1998). The main advantage of using quartz for cosmogenic nuclide studies comes from its abundance in a variety of geological settings (Nishiizumi et al., 1986). Also, its simple target chemistry allows for determination of isotopic production rates that do not vary with its composition (Tuniz et al., 1998).

Production of *in situ* cosmogenic isotopes decreases exponentially with depth and is in general inconsequential below 2 meters depth in rocks (Lal and Peters, 1967). Because of this, ^{10}Be is a good indicator of the near-surface residence time of materials and hence, the rate at which Earth's surface is eroding. In a slowly-eroding basin, sediments will be exposed to cosmic rays for long periods of time, accumulating considerable amounts of cosmogenic nuclides; in contrast, sediments in a more rapidly eroding environment will have a shorter residence time and thus lower cosmogenic nuclide concentrations. As with every method, there are assumptions in the derivation of erosion rate from the measured concentration of cosmogenic nuclides in river sediments.

Assumptions and representativeness of the method

Three published works proposed the use of cosmogenic nuclides in sediments and the assumptions that needed to be met in order for the resulting calculations to be valid:

Brown et al. (1995), Bierman and Steig (1996), and Granger et al. (1996). The following section discusses those assumptions. Representativeness, in time and space, of the measured isotopic concentration is one of them; does the sampled sediment tells the story about the entire basin?. Cosmogenic nuclides assume steady-state erosion rates, which should be representative of erosion over time, but this cannot be confirmed. In terms of spatial representativeness, cosmogenic-derived erosion rates should be representative of the denudation at the sampled watershed and, to a larger extent, of the study area included.

Assessing the delivery processes and geomorphology of the watershed can give insight about the representativeness of a sediment sample. If sediment movement is mostly due to slow creep, the cosmogenic nuclide concentration of material delivered to river channels is likely to be uniform over time and integrate material from the entire basin. On the other hand, if river sediment is mostly supplied by mass-wasting processes like landslides and gullies, sediments may represent episodic events and specific areas of the watershed. Consistency in erosion rates is another factor to consider. If basin-scale erosion is episodically-driven and changes often during the erosional timescale considered, the time it takes to erode a surface material, whether it is a bedrock or sediment layer, sediment is less likely to represent the erosion rates of that timeframe. This can be of significant influence in landscapes that have experienced major climate changes.

Spatial and temporal representativeness of erosion rates in a watershed can be addressed during the sampling. Sediments in old river terraces reflect the erosion rates of the recent past, and provide a basis for interpreting if any sediment input changes has taken place recently (Cox et al., 2009). Nested watershed samples –taken along a river and delineating the sub-basins of the entire watershed- provide information about the spatial change of erosion rates. In a research in Rio Puerco, NM, Bierman and others (2005) observed that variability in erosion rates decreases as the nesting level increases.

Effective mixing, due to bioturbation, landslides and freeze and thaw cycles, helps make river sediment cosmogenic measurements representative of the bedrock and regolith of the entire watershed (Granger et al., 1996) Sediment mixing should reflect an area-weighted average of the pace at which the basin is eroding, assuming that each subwatershed contributes sediment amounts proportional to its long-term erosion rate. That means that an area that is eroding slowly contributes less sediment than an area with a higher erosion rate.

Uniform distribution of quartz in the basin's bedrock is desirable because an uneven distribution will result in biased erosion rates accounting only for quartz-rich areas. It is also important to consider dissolution of minerals due to weathering. Quartz can be considered insoluble, but if the regolith is mostly composed of soluble minerals that will be affected by weathering, cosmogenic nuclide production and measurements will not be representative of the regolith as a whole. Riebe et al., (2001) studied the effect of quartz enrichment on erosion rates constrained from cosmogenic nuclides and

concluded that its effect is negligible. However, he pointed that was the case on temperate weathering environments and that in a tropical scenario its effect is likely to be greater.

Tropical regions cosmogenic studies

Cosmogenic nuclides, as a proxy for erosion rates, have not been widely used in tropical climates. Studies carried out in Sri Lanka (von Blanckenburg, 2004), Madagascar (Cox et. al, 2009), Inter-Andean region (Vanacker et al. 2007) and Puerto Rico (Brown et al., 1995; Brown et al., 1998) are among the few that exist.

Von Blanckenburg and others (2004) conducted research in Sri Lanka with the objective of examining the interactions between weathering, erosion, climate and tectonics. They also assessed chemical weathering from dissolved loads in rivers. Erosion rates ranged between 2 and 45 mm kyr^{-1}. They found that erosion rates in large watersheds increased by a 2-3 fold, as compared to small catchments. This raised the argument that large catchments have two sediment sources: a slow-erosion member and a fast-erosion one. Two potential causes for this difference were discussed: natural geomorphic regimes, and that sediment with low nuclide concentrations is produced in areas of high anthropogenic soil erosion. After comparing their results to a global dataset, they concluded that weathering and erosion are not accelerated by increased temperature and precipitation, but are sensitive to local tectonic forcing.

Long-term denudation rates, modern sediment yields, and land use changes in the Inter-Andean basin in the southern Ecuadorian Andes were quantified and their

relationship was assessed by Vanacker et al. (2007). Denudational mass fluxes averaged 15,000 t km^{-2} yr^{-1}, as determined by cosmogenic nuclides; whereas modern sediment yields obtained from reservoir sedimentation rates averaged 15 × 10^3 t km^{-2} yr^{-1}. Comparing these two, they concluded that removal of surface vegetation cover accelerated erosion rates. If vegetation is reduced significantly in the headwaters, sediment yields can increase by as much as a 100 fold.

Sediment sourcing in Madagascar was studied by Cox and others (2009), using cosmogenic nuclides. ^{10}Be abundances in varied landscape positions were used to fingerprint sediment back to its source. They sampled hillslopes, river sediments, and lavakas, deep-seated gullies common in the Central Highlands of Madagascar. ^{10}Be concentrations in lavaka sediment ranged between 0.8-10 × 10^5 atoms ^{10}Be g^{-1}, and between 6-21 × 10^5 atoms ^{10}Be g^{-1} in colluvium samples. Erosion rates derived from cosmogenic nuclides in river sediment averaged 12 m myr^{-1}. Comparing those abundances, they concluded that lavakas are the dominant source of sediment to rivers (84% by volume), and that they have been since pre-anthropogenic times.

In Puerto Rico, the long-term average denudation rate was found to be ≈ 43 m/Myr for an undisturbed watershed, and approximately 55% of the sediment reached the stream via landslides (Brown et al.,1995). In 1998, Brown and others compared that same watershed to an agricultural one to understand their sediment dynamics. Average long-term denudation for an undeveloped watershed was calculated to be 43 ± 15 m/Myr; and ~85mm ka^{-1} for a mostly agricultural watershed. Sediment discharge samples provided an

estimate of a 750 mm ka^{-1} for the contemporary erosion rate for the agricultural watershed. They attributed the difference in erosion rates to human impacts, specifically agriculture.

Only one cosmogenic study has been carried out so far in Panama. Nichols and others (2005) determined the long-term sediment generation rate in the Upper Rio Chagres Basin. Seventeen river sediment samples were collected, to calculate sediment generation rates in small and steep headwater tributaries, large sub-basins of the Rio Chagres; also a sample was used to assess sediment mixing efficiency and one to determine the average sediment yield of the entire Chagres basin. They found that sediment generation rates are similar in small tributary, large sub-catchments, and the upper Rio Chagres basin as a whole. The average basin-wide sediment generation rate was 275 ± 62 tons km^{-2} y^{-1}, and the weighted average sediment generation rate of the ten tributaries they sampled was 269 ± 63 tons km^{-2} y^{-1}. Such similar rates suggested that sediment mixing is effective in the watershed; there have been no significant sediment storage and/or evacuation events, and that the entire watershed is eroding at a similar pace.

^{10}Be-derived sediment yields were used to assess the lifetime of Lago Alhajuela, the reservoir filling the Panama Canal. Considering the Chagres' basin sediment input alone, the reservoir would fill in ~3,600 years, but when two smaller basins (Boquerón and Pequení) contributing greater amount of sediments, were considered, the reservoir is estimated to fill in ~2,000 years. Both of these smaller basins have experienced

deforestation; the 2- to 3-fold increase in sediment yield, when compared to the Chagres, is attributed to the forest clearing.

Contemporary sediment yields were calculated from suspended sediment records of a station downstream of one of their sampling locations. Using these data, modern sediment yield of the Chagres basin was calculated to be 289 ± 56 tons km^{-2} y^{-1}. Adjacent basins, where land use is dominated by agriculture, showed higher contemporary sediment yields.

Chapter 3- Methods

Basin selection and sampling

Samples presented in my thesis were collected by Russell S. Harmon and Kyle K. Nichols in three field sessions: 2004, 2007 and 2009. The 2004 samples were collected to compare to the sediment dynamics in the Chagres River, the sediment yield of which was measured between 1981 and 1996. The Chagres River is essential to the Panama Canal as it fills one of the main reservoirs that make the canal function. A total of 55 samples were collected, of which 16 were not analyzed for ^{10}Be, due to their low quartz content.

Basins on the eastern side of the Canal were sampled in 2004 to test the human impacts of deforestation. The expectation was to measure long-term erosion rates similar to those estimated for the Chagres River drainage basin. Samples on the northern side of the divide, draining to the Caribbean Sea, were collected to test slope control on erosion. Three rivers in this region were sampled multiple times along their length. These were Rio Nombre de Dios, Cuango and Pequini.

In 2007, samples were collected along the Pan-American Highway north of Panama City. These samples were collected where the road crossed rivers by Kyle K. Nichols. Basins on the northwestern part of the country, and the Pacora River, were sampled by Russell Harmon. Harmon and Steven Goldsmith were conducting research on the chemical weathering in Panama and collected sediment samples as part of that research. Nichols' samples were collected to explore the spatial distribution of erosion in the country and to compare rates of erosion to rates of chemical weathering determined by Harmon and Goldsmith.

In 2009, only four samples were collected. One was a temporal replicate (CHAG2009) for the Rio Chagres, originally sampled in 2002 (Table 3.1). Three landslide-related samples were collected in this trip. One sample was collected from landslide material, one sample upstream from the confluence of the river and the landslide, and one from the river channel downstream of the landslide. These last three samples were then divided into 7 grain size splits, making a total of 21 landslide-related samples.

Laboratory methods

Samples were dried and sieved at Skidmore College. They were sorted by diameter using stackable sieves and a Ro-Tap® Sieve Shaker. Coarse grain-size splits were pulverized using a plate grinder. Landslide-related samples were divided into 7 fractions that were all analyzed for ^{10}Be content: <0.25mm, 0.25-1 mm, 1-2 mm, 2-4 mm, 4-9 mm, 9-12 mm, and >12mm. River sediment samples (unrelated to the landslide) were divided into 3 size fractions: <250 µm, 250-850 µm and >850 µm. Only the 250-850 µm split was chemically treated to isolate quartz and extract ^{10}Be. Other two fractions were saved but not processed.

Samples were chemically treated to isolate the quartz in the Mineral Separation Laboratory at the University of Vermont. This process followed the method published by Kohl and Nishiizumi (1992). Carbonates as well as aluminum and iron oxides were removed in two heated and sonicated etches of 6N HCl. Each etch lasted between 12 and

24 hours; samples were rinsed between etches and fine material was discarded with the solution. After the second etch, samples were rinsed into a tray and dried overnight.

Quartz was purified using repeated dilute hydrofluoric (HF) and nitric (HNO_3) acid etches to eliminate impurities and dissolve acid-soluble minerals. Meteoric ^{10}Be was removed during the sequence of acid etches. Samples were weighed into 4-liter bottles and treated by three 24-hour etches in 1%HF/1%HNO_3 in heated ultrasounds. After the third etch, samples were rinsed, dried, and weighed. After being weighed into 1-liter bottles, samples had two long etches (3 and 7 days) in weak acid (0.5%HF/0.5%HNO_3). Several rinses with deionized water were done after the last etch. No drying was done between the 3 and 7 day etches. After all etches were completes, samples were rinsed, dried, and weighed before storage in 50-ml test tubes. Purity testing was performed at the High-level cosmogenic laboratory to measure native isotopic concentrations in the quartz.

Once the samples were moved to the Cosmogenic Laboratory, a final etch was done to reduce the impurities in the sample and reduce the odds of introducing dust and contamination to the clean-laboratory facilities where ^{10}Be extraction takes place. Samples were weighed in Teflon bottles and enough hydrofluoric acid was added to dissolve the sample in a 5:1 acid to sample ratio by mass. Be and Al carrier were added when weighing in each sample to reach desirable loads (2500 µg Al, and 250 µg Be). The amount of Al carrier added depended on the natural amount of Al in each sample; stable ^{26}Al carrier was added to ensure that at least 2500 µg of aluminum was present in each sample. Digestion took place with increasing heat over the course of two days until the

quartz dissolved completely. Aliquots were removed from the solution before further processing to quantify total (native plus spike) Al in the sample.

Samples were then treated with three perchloric acid dry downs, and two hydrochloric acid dry downs. These prepared the samples for anion columns. In the anion columns, iron is retained and thus removed from the sample. After drying overnight, samples were prepared for cation columns with two drydowns in MilliQ® water with trace sulfuric acid (H_2SO_4), and weak hydrogen peroxide. Chromatography columns for cations were used to separate sample components. Weak sulfuric acid was used to elute the titanium fraction of the samples. Weak HCl (1.2N) was used to strip beryllium from the columns followed by stronger HCl (4N) to remove the aluminum fraction. These fractions were stored until an Inductively Coupled Plasma (ICP) run confirmed that the sample fractions had been successfully separated and no beryllium was lost to the titanium fraction. Samples were dried down overnight, then redissolved and a small yield test aliquot - 50µl for the Al fraction and 200 µl for the Be fraction- was extracted and dissolved in weak sulfuric acid to run on the ICP to confirm successful fraction isolation during cation columns. Titrations with ammonium hydroxide, using methyl red as indicator, neutralized the acid in the sample and precipitated the Al and Be fractions into hydroxide jells. Jells were dried, the BeOH oxidized over a flame to BeO, and the oxide packed into targets after being mixed in a 1:1 molar ratio with niobium (Hunt et al., 2006).

^{10}Be content measuring and erosion rates calculations

Isotopic ratios were measured using Accelerator Mass Spectrometry (AMS) at Lawrence Livermore National Laboratory. Blank corrections were made (as ratio subtractions) based on fully processed blanks that were run with each batch of 12 samples (ten samples and two blanks). Erosion rates based on the isotopic data were obtained using the CRONUS Earth Calculator (http://hess.ess.washington.edu/). To run the calculator, information on effective elevation and latitude is needed, as well as the ^{10}Be content of each sample. Watersheds for each sampling point, based on GPS locations, were delineated in ArcGIS 9.2. A Matlab-based script was run, using the delineated basins, to obtain effective elevation and average latitude of each watershed. These attributes were fed to CRONUS calculator with the isotopic information including the standard to which the Livermore analyses were normalized.

Seventeen samples from the Rio Chagres, which were previously published by Nichols and others (2005) (Table 3.1), were used for statistical analysis. The ^{10}Be concentration for the samples was used as it had been originally published. Erosion rates had been recalculated using CRONUS, and corrected by Portenga and Bierman (2011). These erosion rates were used. Physiographic, seismic, climatic and land use variables were quantified for these subwatersheds in order to include them in statistical analyses.

Erosion rates obtained from CRONUS were highly skewed so they were logarithmically transformed ($\log_{10}$) in order to be able to perform parametric analysis (Figure 3.1). Because no spatial pattern of erosion rates was evident, watersheds were grouped according to their region. Five regions resulted from this clustering:

southwestern region (3 watersheds), northwestern (5 watersheds), central (7 watersheds), central-eastern (8 watersheds), and eastern (17 watersheds). For statistical analysis of the regions, physiographic and climatic parameters for all the watersheds were averaged, except for the number of seismic events, for which the sum of the events in all watersheds was used for parametric analysis.

For calculations and comparison purposes, samples obtained from upstream of the landslide intersection with the stream were combined to simulate a watershed. The following fractions were combined: 0.25-1 mm, 1-2 mm, 2-4 mm, 4-9 mm, and their measured ^{10}Be content were averaged. This clustering resulted in the sampled called "PLS" for which a catchment was delineated, erosion rate calculated and treated as another watershed.

Data Analysis

A Geographical Information System (GIS) was used to quantify variables and study the spatial distribution of erosion rates. All spatial information was projected in NAD 27 Zone 17N (previously denominated Canal Zone). The 90-meter resolution SRTM Digital Elevation Model (DEM) used for watershed delineation and spatial analysis was downloaded from the CGIAR-CSI webpage (http://www.cgiar-csi.org/). There were some gaps of no information on the Panama tiles used for this work. Reclassification of the raster, using the USGS-developed GTOPO30, fixed the gaps. This corrected DEM was used to quantify, slope, area, and relief.

Basins were delineated using ArcHydro Tools in ArcGis 9.2. Watershed delineation was based on the corrected STRM DEM. Several anthropogenic and geomorphic variables were quantified, using spatial statistics, in order to relate them to erosion rate trends. Datasets and their sources are listed in Table 3.2.

Identification of the rock type (s) underlying each watershed was done visually using ArcGIS. For each watershed, all rock types were listed, in order of abundance. The dominant rock type of each watershed was the one used for statistical analysis. Each rock type was assigned a category before statistical testing.

In order to quantify average Peak Ground Acceleration (PGA) for each watershed, Kriging interpolation was used. The downloaded dataset contained a set of points with PGA values. Those were extrapolated to a raster, and the average PGA of each watershed was calculated using zonal statistics.

Data were entered into an SPSS database to run regressions and a multi-variate analysis relating erosion rates to landscape metrics. IBM SPSS Statistics 20 was used for these analyses. A total of 43 variables were quantified in order to relate them to erosion rates; 18 of these variables are bioclimatic. Isothermality is a measure of the annual temperature range experienced on a daily basis (Varela, 2009). It quantifies the oscillation of temperature within a day, as compared to the yearly oscillation. A value of 100 means is interpreted as a site where the diurnal temperature range is the same as the annual temperature range.

The rest of our variables are physiographic and proxies for land use and seismicity. For the landslide samples, only the relationship between grain size and ^{10}Be content was evaluated. To test for significant differences in ^{10}Be concentrations among size groups, they were grouped in four categories. Size fractions smaller than 0.25mm and 0.25-1.0mm were assigned a category (1), samples between 1.0 and 2.0mm were a single category (2). Category 3 was assigned to the fractions 2.0-4.0mm and 4.0-9.0mm; and category 4 was used for samples greater than 9.0mm in diameter.

Comparison to tropical cosmogenic studies

Panamanian erosion rates were compared to other cosmogenic studies in tropical climates, using the erosion rates as re-calculated with CRONUS by Portenga and Bierman (2011). The only samples used for the comparison are the ones that were classified by Tropical in their work. This is important, since some studies originally published data from the same country, but some of the samples are tropical and some are temperate, according to the climate classification used by Portenga and Bierman (2011). Summarized data for these studies are included in Table 3.3

Table 3.1 Rio Chagres published data

Sample ID	Erosion rate (m/Myr)
CCC	154.8
CChC	206.9
CHAG-5	156.6
CHAG-7	97.7
CHAG-9	192.8
CHAG-12	122.9
CHAG-14	88.3
CHAG-15	160.4
CHAG-17	140.5
CHAG-19	163.7
Chico	186.8
CHM-1	125.6
CHT-2	217.6
CLA	177.7
CPC	167.1
CTOM	150.7
PIED	175.1

Samples published in Nichols et al. (2005). These samples are included in the statistical analysis for this research, using the erosion rates as recalculated and standardized by Portenga and Bierman (2011).

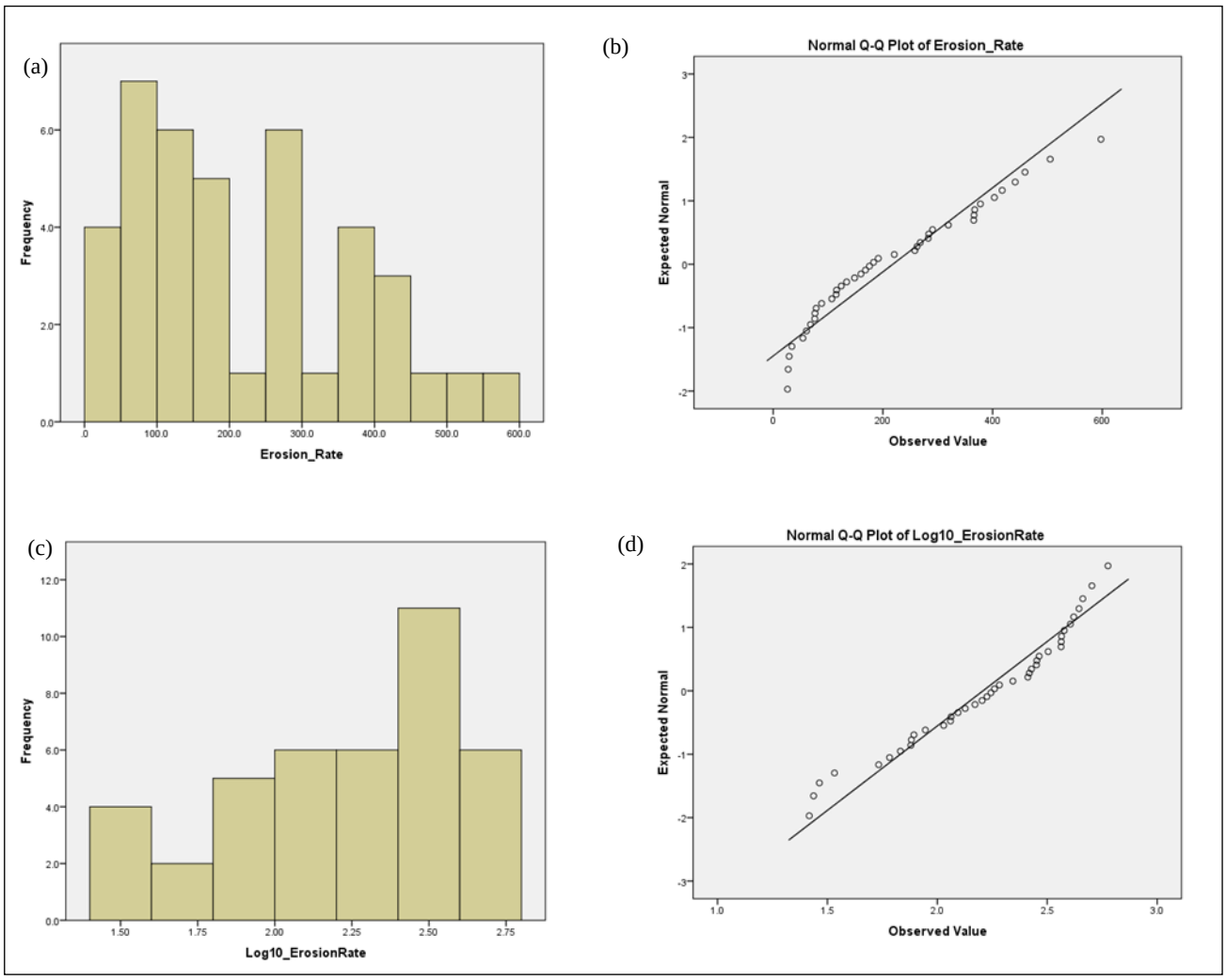

Figure 3.1: Erosion rate distribution. Erosion rates are highly skewed (a) and do not follow a normal distribution (b). Data were logarithmically (base 10) transformed to perform parametric analysis. Skewness in the distribution is reduced after transformation (c) and it approaches a normal distribution (d).

Table 3.2 Spatial datasets and source

Dataset	Source
Digital Elevation Model	Consultative Group on International Agricultural Research- Consortium for Spatial Information (CGIAR-CSI) (http://srtm.csi.cgiar.org/SELECTION/inputCoord.asp)
Forest Cover	Global Land Cover Facility (http://glcf.umiacs.umd.edu/data/treecover/)
Seismic Catalog	Instituto de Geociencias (Personal communication)
Climatic data	WorldClim (http://www.worldclim.org/formats)
Geology	Smithsonian Tropical Research Institute (http://mapserver.stri.si.edu/geonetwork/srv/en/main.home)
Global Seismic Hazard Map	Global Seismic Hazard Assessment Program (http://www.seismo.ethz.ch/static/GSHAP/global/)

Summarized isotopic data and erosion rates for previously published cosmogenic studies in tropical regions. Erosion rates were obtained from Portenga and Bierman (2011) published recalculated data and averaged. The standard deviation of all watersheds in each study is expressed as the error of the average erosion rate

Table 3.3 Cosmogenic nuclide-derived erosion in tropical climates

Published work	Study Site	Erosion rate (m/Myr)	Watersheds in study (n)
Brown et al., 1995	Puerto Rico	61.7 ± 41.3	8
Brown et al., 1998	Puerto Rico	60.4 ± 31.9	166
Cox et al. 2009	Madagascar	13.9 ± 5.7	4
Hewawasam et al., 2003	Sri Lanka	21.1 ± 4.2	6
Von Blackenburg et al., 2004	Sri Lanka	16.2 ± 7.0	10

Summarized isotopic data and erosion rates for previously published cosmogenic studies in tropical regions. Erosion rates were obtained from Portenga and Bierman (2011) published recalculated data and averaged. The standard deviation of all watersheds in each study is expressed as the error of the average erosion rate

Chapter 4- Results

This section presents my findings for both river sediment and landslide material samples. Erosion rates vary widely from one geographical region to another. Isotopic concentration in landslide-related material varies as a function of grain size.

River sediment samples

The concentration of *in situ* ^{10}Be measured in Panamanian river sand varies widely from 7.4 ± 1.6 to 139 ± 3 × 10^3 atoms/g (Table 4.1). When samples were grouped by region, quartz extracted from rivers in the southwestern region had the lowest ^{10}Be concentration (8.37 ± 1.27 × 10^3 atoms/g). The lowest concentration of ^{10}Be measured as part of this project was in the river sediment of the Rio Bartolo (BART), in that region (Table 4.2 and Figure 4.1). Samples from the central-eastern region had an average ^{10}Be concentration of 64.0 ± 46.6 × 10^3 atoms/g. This variance in the central-eastern region was the largest of all regions (72% SD). The mean ^{10}Be concentration was significantly different between the eastern and central-eastern region ($p = 0.007$) but no significant differences were found in mean ^{10}Be concentrations for stream sediment from other regions (Table 4.2 and Figure 4.1).

Erosion rates, inferred from the concentration of *in situ* produced ^{10}Be range from 26.1 m/Myr to 597 m/Myr; the average rate for the 35 rivers we sampled is 218 m/Myr ± 151 m/Myr, the area weighted average is 150 m/Myr, and the median erosion rate is 179 m/Myr (see Table 4.1). There are no general trends in erosion rates, however, the most

slowly eroding basins are found in the central-eastern region, and rapidly eroding basins scattered through the country (Fig. 4.2). When samples were grouped by region, the southwestern region had the highest average erosion rates (Table 4.3); however, the central region has the biggest variance in erosion rates (Figure 4.3). Average erosion rate for the southwestern region is significantly different from the average erosion rate of the central ($p = 0.020$) and central-eastern regions ($p = 0.003$). All other differences were not significant.

Two rivers, the Pequini and Chagres were sampled multiple times along their length to assess spatial variations in erosion (Figure 4.4). A sample representing the Pequini headwaters (PHW) was 7..40km away from the sample extracted before the confluence of the Pequini with the Rio San Miguel (PSM), and 13.3km away from a sample taken at the outlet of the watershed (PLA). Erosion rates calculated for the three nested watersheds showed a 13 percent standard deviation (Table 4.4). The Rio Chagres was sampled in 2009 (CHAG2009), and so was a landslide on the Chagres watershed. Amalgamated samples from upstream of the landslide were combined to represent a sediment sample (PLS) that encloses the watershed for CHAG2009. Erosion rates calculated for both segments of the Rio Chagres (PLS and CHAG2009) differed by a percent standard deviation of 71.

For two rivers, there are temporal replicates, that is, a sample was collected from a similar location but at a different time (see Figure 4.4). The Rio Nombre de Dios was sampled in 2004 (NDD) and 2007 (DIOS), and so was the Rio Cuango (CUAN, 2004;

CNGO, 2007). The smaller variation between nested watersheds was found in the Rio Nombre de Dios, where the variance is 6%. Rio Cuango has a slightly bigger difference, 23%. Erosion rates were calculated for the area between subcatchments (Table 4.5). In general, ^{10}Be content and erosion rates of the subwatersheds were similar (see Table 4.4).

In general, bivariate linear regression analysis showed few statistically significant relationships between ^{10}Be-inferred basin scale erosion rates and landscape scale variables (Table 4.6). There were no significant relationships between erosion rates and physiographic metrics (area, slope, and relief). Several bioclimatic variables showed weak but positive relationships with erosion rates including temperature seasonality (R^2= 0.445, p= 0.004), and precipitation during both the driest month (R^2= 0.319, p= 0.045) and the driest quarter (R^2= 0.376, p= 0.017). Two bioclimatic variables showed weak negative relation to erosion rates: isothermality (R^2= 0.381, p= 0.015) and precipitation seasonality (R^2= 0.394, p= 0.012).

The strongest relationships with seismicity are negative. The average magnitude of seismic events showed a relationship at a 75km buffer from the watersheds (R^2= 0.550, p<0.005) and at the 25km buffer (R^2= 0.431, p= 0.005). Within a 50km buffer, the strongest relation was found between erosion rates and the average depth of the events (R^2= 0.466, p= 0.002). Other weak relationships were found with the 25km, 50km, 75km and 100km buffers. No significant relationships were found at the 100m and only one at the 10km distance (Table 4.7). Tree cover is also negatively related to erosion rates (R^2=

0.351, p= 0.026). There is a strong relationship between physical and chemical weathering in Panamanian watersheds (R^2 = 0.558, p= 0.021, n = 9). Stepwise regression results in a model that includes both chemical weathering and precipitation of the driest month as explanatory variables (R^2=0.915, p= 0.001).

Although erosion rates and landscape scale parameters are not well correlated at the basin scale, they are better correlated if considered at a regional scale (Figures 4.5 and 4.6). Clustering samples into regions and assessing their relationship to parameters, shows an increase in correlation coefficients, except for mean annual precipitation, which decreases (see Table 4.6). However, the small number of regions (n = 5) translates in high p-values for the regressions, suggesting that the relationships are not statistically significant at $p < 0.1$.

Landslide samples

^{10}Be concentration in the grain size splits of sediment collected from an active landslide as well as up and down stream of the slide ranged from 7.33 ± 0.40 to 39.1 ± 1.71 × 10^3 atoms/g, on the low end of concentrations measured as part of this study (Table 4.8). Grain size and *in situ* ^{10}Be concentration are inversely related (Fig. 4.7). Individual linear regressions showed that they are well correlated (R^2= 0.600; $p < 0.005$). The isotopic concentration of the landslide material is less than that for the upstream and downstream material, in all size fractions. There are only three samples for each fraction. Because of this, it is not statistically possible to test for differences in isotopic concentration for each of the fractions.

Sediment upstream of the landslide contains more ^{10}Be than sediment downstream. Analysis of Variance showed that the relationship between ^{10}Be content and grain size is statistically significant ($F = 4.175$; $p = 0.013$). When several size fractions are grouped and categorized, a stronger relationship is found ($F=9.536$, $p = 0.001$). Mean isotopic concentration of the <0.25mm fraction is statistically different from all the fractions greater than 2.00mm at the 0.05 level. No relationship holds between ^{10}Be concentration and sediment source ($F= 2.193$; $p = 0.141$), but there is an evident difference in their average content (Figure 4.8). A component mixing model (upstream and landslide sediment) suggests that the landslide accounts for 50% of the sediment just downstream of the slide.

Table 4.1: Samples locations and isotopic data

Sample ID	Northing	Easting	^{10}Be content (x 10^3 atoms/g)	Erosion rate (m/Myr)
ANT	928349	581595	22.7 ± 0.8	175 ± 7
BART	916325	296212	7.4 ± 1.7	505 ± 120
BLA	1035402	657862	15.1 ± 1.3	258 ± 22
C-NATA	919929	553005	137.0 ± 2.6	27.4 ± 0.5
CAIM	984975	637879	95.4 ± 1.8	34.1 ± 0.7
CAPI	964402	622520	34.8 ± 0.7	115 ± 2
CHAG2009	1034979	689087	68.1 ± 1.7	60.6 ± 1.6
CHAME	947518	622722	23.7 ± 2.0	168.2 ± 14.2
CHAN	1035839	331670	39.4 ± 1.2	160 ± 5
CHVIE-H	978626	324237	36.1 ± 1.3	284 ± 10
CNGO	1056452	685595	14.3 ± 1.2	262 ± 22
COBRE	908408	457641	51.7 ± 2.2	75.8 ± 3.4
CORO	913112	293805	7.9 ± 0.6	459 ± 33
CUAN	1053293	688405	10.5 ± 0.8	366 ± 29
CUL	1052186	692279	13.1 ± 1.0	291 ± 23
DIOS	1057813	666135	8.3 ± 1.7	441 ± 92
FELIX	914518	405028	8.0 ± 0.8	597 ± 62
GLOR	993157	364491	35.4 ± 1.5	124 ± 5
GRUMO	989538	369257	17.6 ± 1.0	283 ± 16
GUAN	911892	293354	9.8 ± 1.2	367 ± 46
GUI	931896	602809	18.1 ± 0.6	221 ± 8
IND	993439	590052	66.4 ± 1.8	54.1 ± 1.5
MAND	1044547	700401	19.6 ± 0.7	192 ± 7
MARIA	899354	534672	55.6 ± 1.3	68.0 ± 1.6
NDD	1058344	666294	9.0 ± 1.4	403 ± 62
PACORA	1003367	688077	10.9 ± 0.5	366 ± 18
PAN02	1041964	722329	31.7 ± 0.9	116 ± 3
PAN06	1017356	777490	36.1 ± 0.9	107 ± 3
PERE	975402	625864	112.4 ± 2.1	29.1 ± .6
PHW	1043899	671363	10.5 ± 1.5	378 ± 56
PLA	1035529	660978	9.4 ± 0.6	417 ± 28
PLS	684394	1035285	23.2 ± 0.7	183 ± 6
PSM	1038574	666242	12.4 ± 0.9	319 ± 24
ROBO	997213	356281	30.5 ± 0.9	148 ± 5
SAJ	960284	624479	138.7 ± 3.1	26.1 ± 0.6
SAN-T	1025128	678293	57.6 ± 1.4	76.2 ± 1.9

SANPAB	906069	472211	31.8 ± 0.7	134 ± 3
SMP	1038660	666261	14.5 ± 1.7	268 ± 33
TABA	907203	435575	61.9 ± 2.5	78.2 ± 3.2
VIGUI	906818	438230	50.1 ± 1.5	88.2 ± 2.6

Sample locations are based in NAD 27-Canal Zone. Measured ^{10}Be in the samples is expressed in 1,000 atoms/g. CRONUS Earth Calculator was used to calculate erosion rates. The internal uncertainty calculated by CRONUS is expressed as the uncertainty of each erosion rate. Isotopic data standardized to KNSTD2007 with assumed ratio at 2850×10^{-15}

Table 4.2: ^{10}Be concentration for each region

Region	Average ^{10}Be (x 10^3 atoms/g)	Range ^{10}Be (x 10^3 atoms/g)	Standard deviation
Southwest (n= 3)	8.37	7.40 – 9.80	1.27
Northwest (n= 5)	31.80	17.60 – 39.40	8.55
Central (n= 7)	56.59	8.00 – 137.00	39.87
Central-East (n= 8)	64.03	18.10 – 138.70	46.60
Eastern (n= 17)	18.68	8.30 – 68.10	14.99

Average isotopic concentration for each region, presented in 1,000 atoms/g. Range column shows the minimum and maximum ^{10}Be concentration for the watersheds in each region.

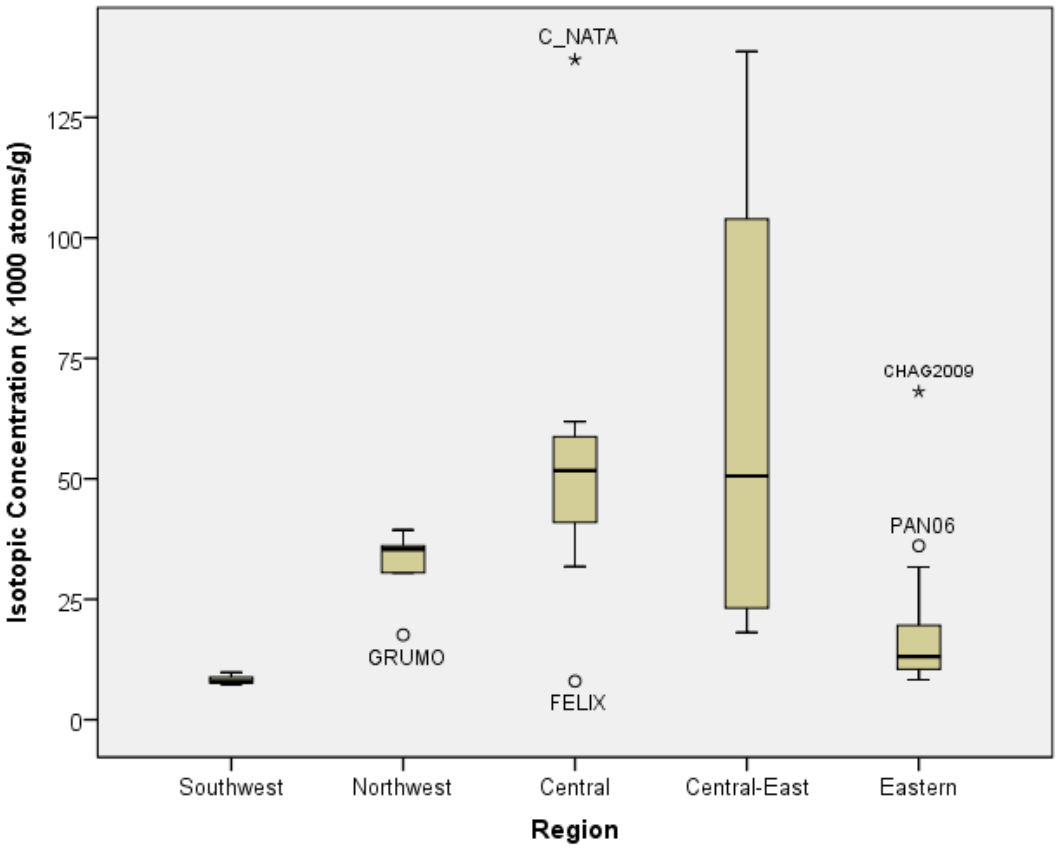

Figure 4.1: Difference in isotopic concentration among regions. Lines in the boxes represent the median of each region. Circles outside of the whiskers are outliers, and the asterisks represent extreme values in the dataset.

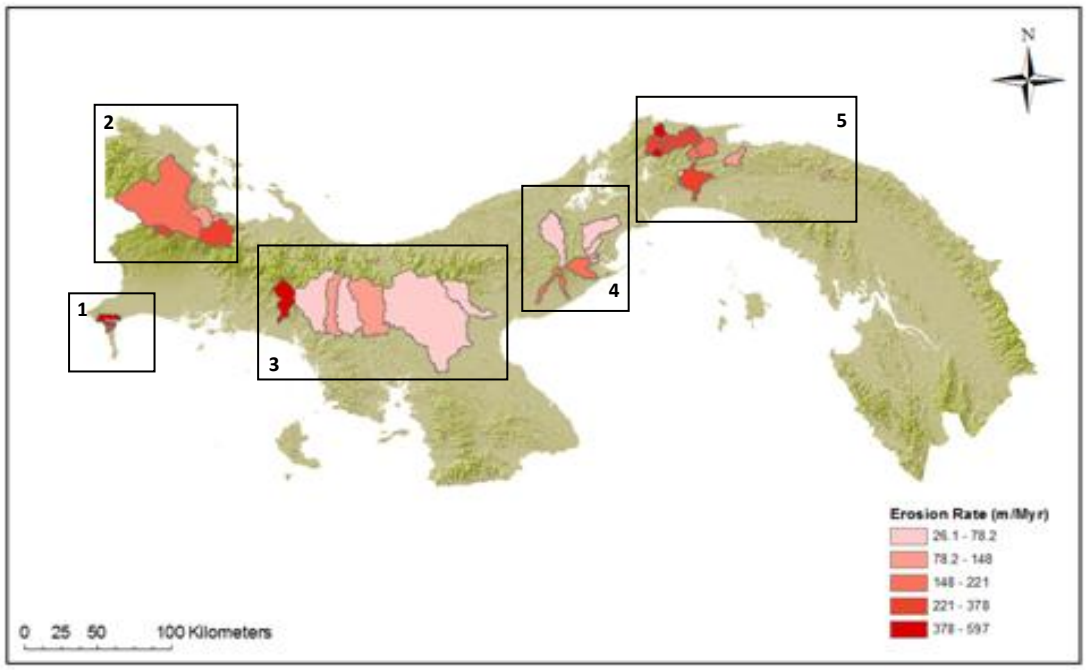

Figure 4.2: Spatial distribution of erosion rates. There is no spatial pattern on the erosion rates across Panama. Some fast-eroding watersheds are scattered through the country. For regional analysis, samples were divided into 5 groups: Southwestern (box 1), Northwestern (2), Central (3), Central-East (4), and Eastern (5). When ANOVA was performed on regional analysis, each region had the number assigned in this figure.

Table 4.3: Average erosion rates and area for each region

Region	**Average erosion rate (m/Myr)**	**Average area (km^2)**
Southwestern (n= 3)	444 ± 70	34 ± 28
Northwestern (n= 5)	200 ± 77	476 ± 752
Central (n= 7)	153 ± 199	783 ± 815
Central-east (n= 8)	103 ± 77	142 ± 141
Eastern (n= 17)	264 ± 151	84 ± 64

Erosion rates and area for each region were averaged, and the standard deviation was calculated and is expressed as the standard deviation of the measurements. The number of watersheds in each region is in parenthesis on the first column.

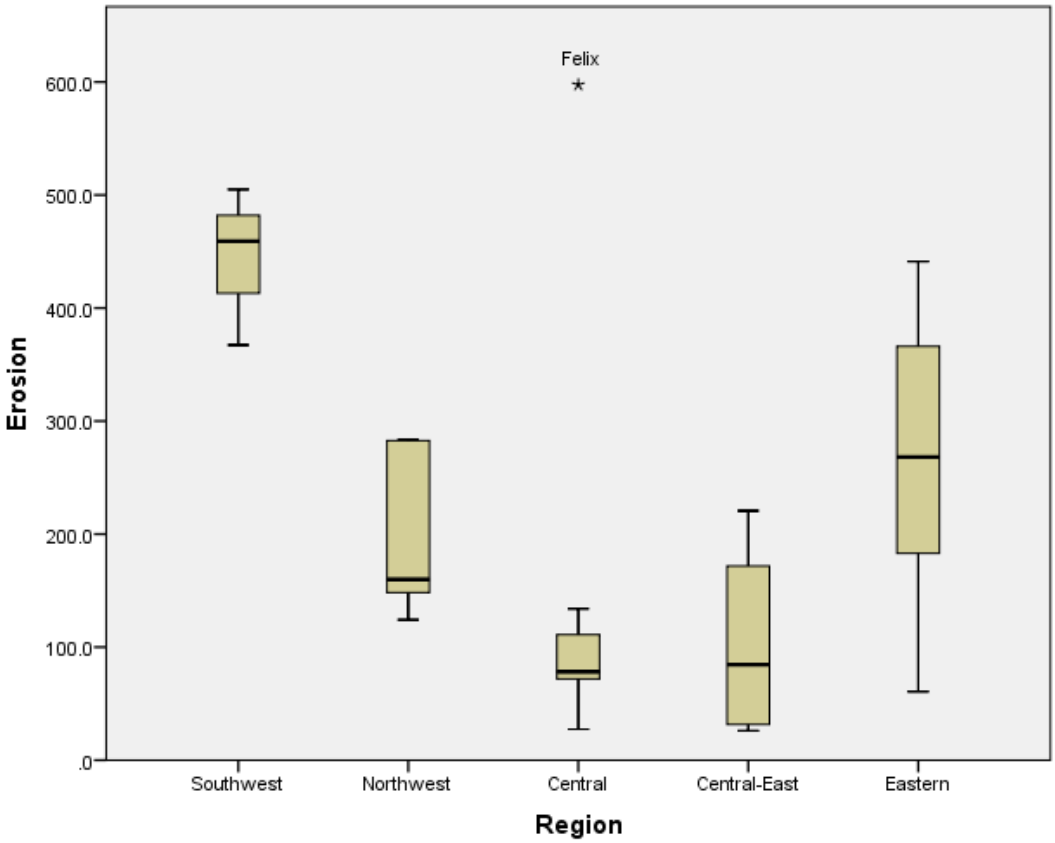

Figure 4.3: Average erosion by region. The lines inside the boxes represent the median of each region. Horizontal lines in the bars represent the minimum and maximum values for each region. The southwestern region hast the highest average erosion rate, and the central region has the highest variability. Rio Felix, represented by an asterisk, is an extreme outlier in our dataset.

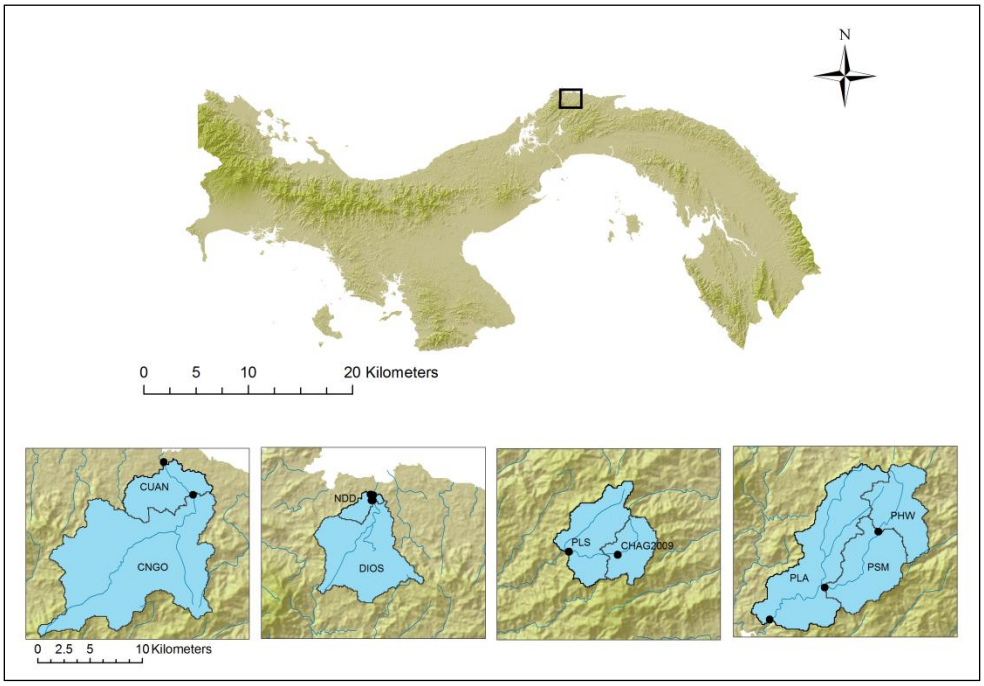

Figure 4.4. Spatial replicate samples. Nested watersheds for rivers that sampled more than once along their length: Rio Cuango (a), Rio Nombre de Dios (b), Rio Chagres (c), and Rio Pequini (d). Black dots represent the sample locations. Black box outlines the area where all nested watersheds are located.

able 4.4: Nested watersheds summarized data

River	Sample name	Distance between samples (km)	Sample collection year	^{10}Be concentration ($\times 10^3$ atoms/g)	Erosion Rate (m/Myr)	% SD erosion rates within each river	Subwatershed area (km^2)
Nombre de Dios	NDD	0.55	2004	9.0 ± 1.4	403 ± 62	6	62.46
	DIOS		2007	8.3 ± 1.7	441 ± 92		56.6
Cuango	CNGO		2007	14.3 ± 1.2	262 ± 22		27.49
	CUAN	4.20	2004	10.5 ± 0.8	366 ± 29	23	142.04
Pequini	PHW		2004	10.5 ± 1.5	378 ± 56		34.21
	PLA	13.3 (PHW-PLA)	2004	9.4 ± 0.6	417 ± 28		35.14
	PSM	7.40 (PHW-PSM)	2004	12.4 ± 0.9	319 ± 24	13	76.06
Chagres	CHAG2009	4.7 (CHAG2009-PLS)	2009	68.1 ± 1.7	60.6 ± 14.2		21.27
	PLS		2009	23.2 ± 0.7	183 ± 68	71	56.57

Distances were measured in ArcGIS. Percent standard deviation was calculated for each river. Area for each subwatershed was calculated based on a 90-m SRTM DEM using Matlab.

Table 4.5: Erosion rates for the region within subwatersheds

River	Sample Name	Erosion Rate (m/Myr)	Subwatershed Area (km^2)	Erosion between Watersheds (m/Myr)
Nombre de Dios	NDD	403 ± 62	58.60	215
	DIOS	441 ± 92	53.05	
Cuango	CNGO	262 ± 22	158.05	-269
	CUAN	366 ± 29	132.18	
Chagres	CHAG2009	60.6 ± 14.2	20.11	250
	PLS	183 ± 68	56.57	
Pequini (A)	PHW	378 ± 56	32.06	270
	PSM	319 ± 24	70.76	
Pequini (B)	PSM	319 ± 24	70.76	509
	PLA	417 ± 28	146.18	
Pequini (C)	PHW	378 ± 56	32.06	428
	PLA	417 ± 28	146.18	

Erosion rates for the area between subwatersheds were calculated using the equation presented by Granger et al. (1996): $E_{2\text{-}1} = E_2A_2 - E_1A_1 / A_2 - A_1$.

Table 4.6: Regressions and ANOVA results

Variable	R^2 (n=40)	R^2 (n=5)
Slope	*0.009 (p=0.955)*	*0.192 (p=0.460)*
Area	*0.223 (p= 0.166)*	*0.267 (p=0.372)*
Relief	*0.196 (p= 0.226)*	*0.353 (p=0.290)*
Elevation	*0.040 (p= 0.805)*	*0.186 (p=0.468)*
Average Temperature	*0.041 (p= 0.800)*	*0.071 (p=0.666)*
Isothermality	0.381 (p= 0.015)	*0.164 (p=0.499)*
Temperature Seasonality	0.445 (p= 0.004)	*0.419 (p=0.237)*
Max Temp Warm Month	*0.066 (p= 0.686)*	*0.160 (p=0.504)*
Min Temp Cold Month	*0.005 (p= 0.676)*	*0.004 (p=0.921)*
Temperature Range	*0.019 (p= 0.907)*	*0.270 (p=0.369)*
Temperature Wet Quart	*0.074 (p= 0.648)*	*0.074 (p=0.658)*
Temperature Dry Quart	*0.037 (p= 0.823)*	*0.060 (p=0.692)*
Temperature Warm Quart	*0.026 (p= 0.876)*	*0.076 (p=0.654)*
Temperature Cold Quart	*0.084 (p= 0.605)*	*0.046 (p=0.728)*
Annual Precipitation	*0.307 (p= 0.054)*	*0.000 (p=0.973)*
Mean Diurnal Range	*0.055 (p= 0.737)*	*0.156 (p=0.511)*
Precipitation Wet Month	*0.048 (p= 0.771)*	*0.450 (p=0.215)*
Precipitation Dry Month	0.319 (p= 0.045)	*0.000 (p=0.981)*
Precipitation Seasonality	0.394 (p= 0.012)	*0.003 (p=0.936)*
Precipitation Wet Quart	*0.045 (p= 0.784)*	*0.083 (p=0.638)*
Precipitation Dry Quart	0.376 (p= 0.017)	*0.003 (p=0.928)*
Precipitation Warm Quart	*0.292 (p= 0.068)*	*0.005 (p=0.913)*
Precipitation Cold Quart	*0.023 (p= 0.889)*	*0.027 (p=0.792)*
Tree Cover	0.351 (p= 0.026)	*0.417 (p=0.239)*
Chemical Weathering	0.726 (p= 0.004)	-
Peak Ground Acceleration	0.307 (p= 0.054)	*0.589 (p=0.130)*
Surface Geology	*F = 2.427 (p= 0.102)*	-
Seismic Events 100m	*0.184 (p= 0.256)*	*0.392 (p=0.258)*
Average Depth 100m	*0.128 (p= 0.430)*	*0.028 (p=0.786)*
Average Magnitude 100m	*0.155 (p= 0.340)*	*0.074 (p=0.658)*
Seismic Events 10km	0.338 (p= 0.033)	0.813 (p=0.036)
Average Depth 10km	*0.140 (p= 0.389)*	*0.302 (p=0.338)*
Average Magnitude 10km	*0.220 (p= 0.172)*	*0.196 (p=0.456)*
Seismic Events 25km	0.350 (p = 0.027)	*0.474 (p=0.199)*
Average Depth 25km	0.334 (p = 0.035)	*0.477 (p=0.196)*
Average Magnitude 25km	0.431 (p = 0.005)	*0.679 (p=0.086)*

Seismic Events 50km	0.363 (p = 0.021)	*0.706 (p=0.075)*
Average Depth 50km	0.466 (p = 0.002)	*0.450 (p=0.215)*
Average Magnitude 50km	0.368 (p = 0.019)	*0.173 (p=0.486)*
Seismic Events 75km	0.348 (p = 0.028)	*0.389 (p=0.157)*
Average Depth 75km	0.420 (p = 0.007)	*0.390 (p=0.260)*
Average Magnitude 75km	0.550 (p = 0.000)	*0.407 (p=0.247)*
Seismic Events 100km	0.316 (p= 0.047)	*0.179 (p=0.478)*
Average Depth 100km	0.198 (p= 0.221)	*0.286 (p=0.354)*
Average Magnitude 75km	0.550 (p = 0.000)	*0.407 (p=0.247)*
Seismic Events 100km	0.316 (p= 0.047)	*0.179 (p=0.478)*

All parametric analyses were performed with $\log_{10}$ transformed erosion data. Fields in italics represent relationships that are not statistically significant at the 0.05 significance level. For regional analysis, the number of seismic events is the sum of the events in all watersheds. For all other parameters, values were averaged. No analysis was done for surface geology at the regional scale, because only two categories were present when samples were grouped. Sedimentary rocks are not represented. No chemical weathering analysis was done at the regional scale. The 9 watersheds that have silicate weathering data are not representative of all regions.

Table 4.7 Seismicity measured at various buffers.

Variable	R^2	p	Slope
Events 100m	*0.184*	*0.256*	*0.006*
Depth 100m	*0.128*	*0.760*	*-0.002*
Magnitude 100m	*0.155*	*0.340*	*-0.026*
Events 10km	0.338	0.033	0.001
Depth 10km	*0.140*	*0.389*	*-0.001*
Magnitude 10km	*0.220*	*0.172*	*0.050*
Events 25km	0.350	0.027	0.001
Depth 25km	0.334	0.035	-0.005
Magnitude 25km	0.431	0.005	-0.165
Events 50km	0.363	0.021	0.000
Depth 50km	0.466	0.002	-0.008
Magnitude 50km	0.368	0.019	-0.361
Events 75km	0.348	0.028	0.0000
Depth 75km	0.420	0.007	-0.012
Magnitude 75km	0.550	0.000	-1.359
Events 100km	0.316	0.047	0.000
Depth 100km	*0.198*	*0.221*	*-0.006*
Magnitude 100km	0.352	0.026	-1.080

Fields in italics represent relationships that are not statistically significant at the 0.05 significance level. The slope of the line is presented.

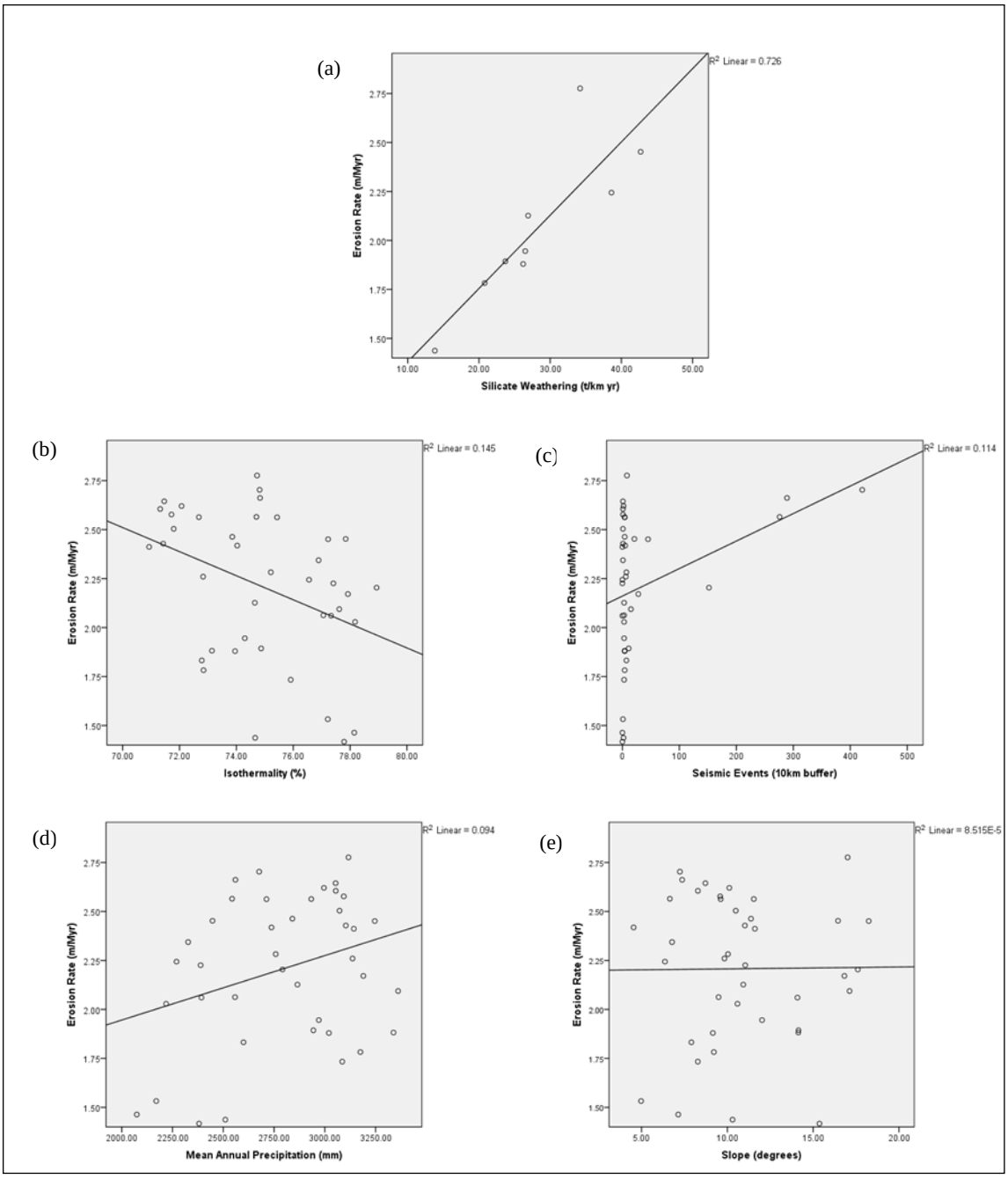

Figure 4.5: Country-scale bivariate analysis. The relationship between erosion and silicate weathering was the strongest found in our data (a). Isothermality (b) and seismic events within a 10km buffer (c) hold a statistically significant relation to erosion, but it is weak. Mean annual precipitation (d) and slope (e) are not related to erosion rates.

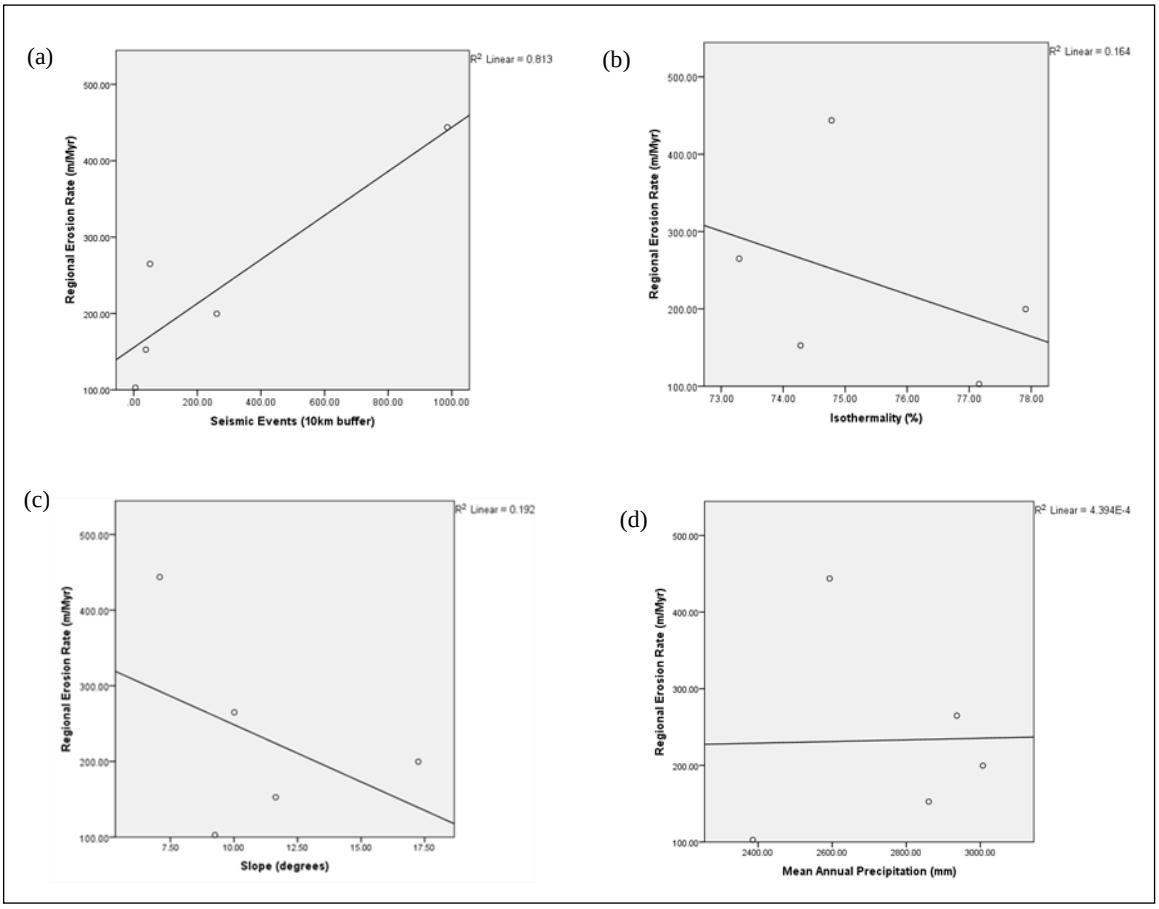

Figure 4.6: Regional-scale bivariate analysis. The only significant relationship found at the regional scale is between erosion and seismic events within a 100km buffer (a). Isothermality (b) and slope (c) show a greater correlation to erosion than at the country scale. However, none of them is significant (see table 4.6). The strength of the relationship between mean annual precipitation and erosion (d) decreases at the regional scale. It is not statistically significant.

Table 4.8: Isotopic concentration in landslide fractions

Sample ID	Northing	Easting	^{10}Be content (x 10^3 atoms/g)
PLSU <0.25 mm	684394	1035285	39.1 ± 0.6
PLSU 0.25-1 mm	684394	1035285	34.9 ± 0.7
PLSU 1-2 mm	684394	1035285	26.3 ± 0.8
PLSU 2-4 mm	684394	1035285	18.0 ± 0.6
PLSU 4-9 mm	684394	1035285	13.6 ± 0.7
PLSU 9-12 mm	684394	1035285	13.3 ± 0.1
PLSU >12 mm	684394	1035285	9.5 ± 0.5
PLSS <0.25 mm	684394	1035285	12.8 ± 0.2
PLSS 0.25-1 mm	684394	1035285	17.2 ± 0.5
PLSS 1-2 mm	684394	1035285	14.1 ± 0.5
PLSS 2-4 mm	684394	1035285	11.0 ± 0.7
PLSS 4-9 mm	684394	1035285	10.4 ± 0.6
PLSS 9-12 mm	684394	1035285	9.4 ± 0.5
PLSS >12 mm	684394	1035285	7.8 ± 0.4
PLSD <0.25 mm	684394	1035285	36.3 ± 0.8
PLSD 0.25-1 mm	684394	1035285	30.2 ± 0.8
PLSD 1-2 mm	684394	1035285	20.3 ± 0.8
PLSD 2-4 mm	684394	1035285	13.7 ± 0.6
PLSD 4-9 mm	684394	1035285	11.4 ± 0 .7
PLSD 9-12 mm	684394	1035285	10.8 ± 0.9
PLSD >12 mm	684394	1035285	7.3 ± 0.4

GPS locations are the same for all samples. Sample locations are based on NAD-27 Canal Zone.
Measured ^{10}Be concentration shown in 1,000 atoms/g.

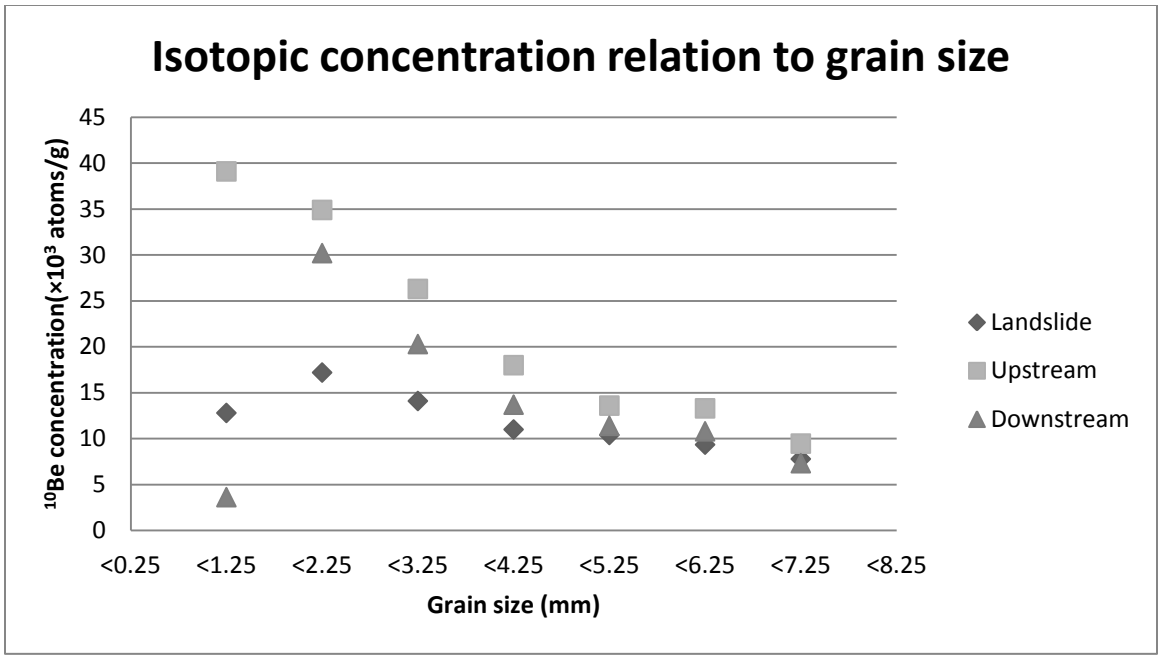

Figure 4.7: Isotopic concentration variation with grain size. Two general trends can be identified from the grain size fractions of our data. First, ^{10}Be concentration decreases as grain size increases. Also, material from the landslide (PLSS) almost always has the lowest isotopic concentration of each grain size fraction.

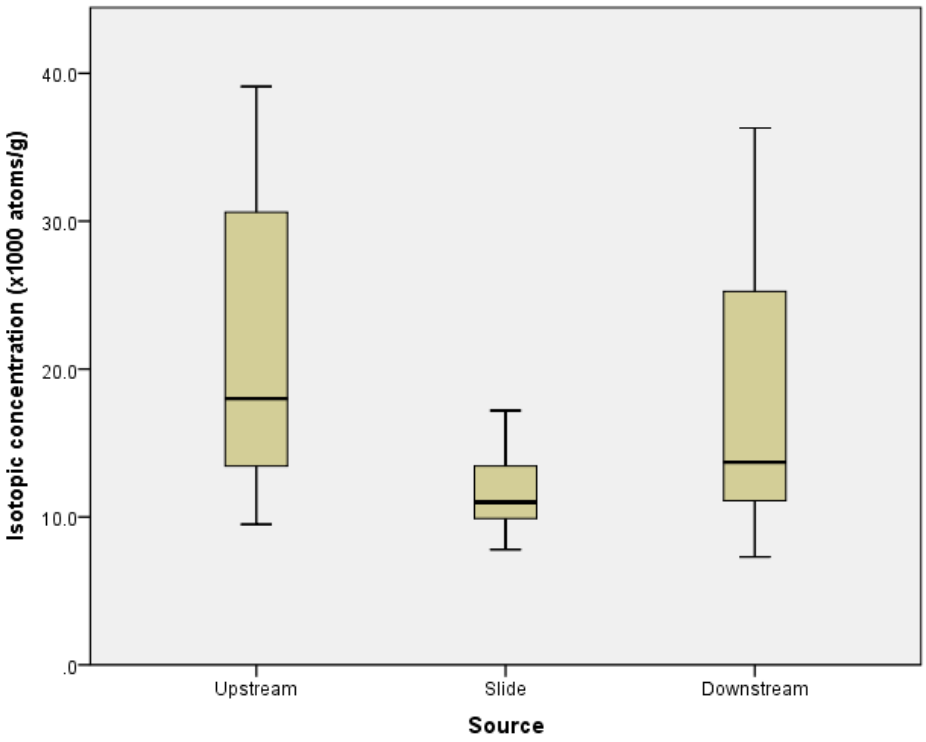

Figure 4.8 Variation of isotopic concentration according to material source. Median of each group is represented by the lines inside the boxes. Minimum and maximum are the horizontal lines in the whiskers. Landslide material showed the lowest concentration of ^{10}Be when compared to material up and downstream. No statistical testing showed the difference in isotopic concentration, according to sediment source.

Chapter 5 - Discussion

Basin-scale erosion rates in Panama vary over more than an order of magnitude and are in general, quite rapid, averaging several hundred meters per million years. Erosion rates appear unrelated to topographic metrics, vary in a coherent spatial pattern, and are correlated to various expressions of tectonic activity. Our dataset suggests that physical erosion rates and chemical weathering of silicate rocks are well correlated.

Comparison to other tropical cosmogenic studies

Erosion rates of Panamanian basins span much of the range previously reported for tropical basins. Forty watersheds in Panama, some of which are nested and vary in area from 13.6 km^2 to 2,410 km^2, had erosion rates that range from 26.1 ± 0.6 m/Myr to 597 ± 62 m/Myr. The average erosion rate for the Panamanian watersheds considered in this study is significantly different from that of published data from other tropical study sites including Puerto Rico, Madagascar, and Sri Lanka ($F=19.767$, $p< 0.005$). Watersheds included in those tropical studies, ranged in area from 0.02 to 134.6 km^2 with most under 50 km^2. Panama's dataset is robust when compared to other tropical studies; the number of samples included in those studies ranges from 4 to 10, whereas the Panama dataset has 40 watershed samples (Figure 5.1).

Denudation rates have been determined in three rivers in Puerto Rico, in two separate studies. Brown and others (1995) determined an average erosion rate of 61.7 ± 41.34 m/Myr for the Rio Icacos. In 1998, Brown et al. determined the erosion rates for the Quebrada Guabá and Rio Cayaguás, the erosion rate for the first was 50.8 ± 27.7

m/Myr and 70.1 ± 19.9m/Myr for the latter. Average erosion rates in tropical Madagascar (n = 4) are 13.9 ± 5.7 m/Myr, as determined by Cox et al. (2009). Two separate studies have constrained cosmogenically-derived erosion rates in Sri Lanka. In 2003, Hewasam et al. found that the average erosion rate of six tropical subwatersheds of the Upper Mahaweli catchment was 21.1 ± 4.2 m/Myr. von Blanckenburg et al. (2004) report an average erosion rate of 16.2 ± 7.0 m/Myr in Sri Lanka (n=16).

When compared to these study sites, Panama is eroding faster than all of them. Seismicity and tectonic setting differ between Panama, Madagascar, and Sri Lanka; the latter two are located in a region with no tectonic activity. In contrast, Panama is located in an active tectonic zone. Madagascar also has little tectonic activity. Peak ground acceleration, defined as the magnitude of ground motion with a 10% chance of being exceeded within 50 years, was estimated to be 0.06 g for the 16 studied watersheds Sri Lanka, and 0.36 for Madagascar (Portenga and Bierman, 2011). For Panama, mean peak ground acceleration in the 40 studied watersheds, is more than an order of magnitude higher, ranging between 1.77 and 4.37 g (average: 2.29). In Puerto Rico, peak ground acceleration averaged 1.88.

Mean temperature in the sampled Panamanian watersheds averaged 24.4 °C; in Sri Lanka, it averaged 19.2°C, in Madagascar, 20.2°C and 21.6°C in Puerto Rico. Mean annual precipitation for the watersheds is relatively similar in Panama, Puerto Rico and Sri Lanka, averaging 2796 mm, 2599 mm and 2480 mm respectively. They differ from Madagascar, where it averages 1134mm.

Relation to silicate weathering

The strongest and most significant relationship in our dataset was found between erosion rates and chemical weathering of silicate rocks (R^2= 0.726, p= 0.004, n= 9). A positive relationship between chemical and physical erosion has been found before. In some cases, specifically silicate weathering has been studied.

In their study of the controls on chemical weathering in a variety of climate regimes, Riebe et al. (2004) argued that there is a potential positive feedback between physical and chemical erosion. Physical erosion may depend on the chemical breakdown and weakening of rocks as minerals alter, and chemical weathering depends on the availability of fresh mineral surfaces created by physical erosion. In a study looking at physical erosion and chemical weathering in Rio Icacos (Puerto Rico), Riebe et al (2003) concluded that there is a tightly coupled relationship between physical erosion and chemical weathering. Von Blanckenburg (2005) also found that physical erosion and chemical denudation are tightly related. That study compiled previously published isotopic data and related it to physiographic metrics and chemical weathering data. He found that the slope of the best fit line on the plot of chemical versus physical erosion rates was 0.2. For Panama, we compared chemical and physical denudation and we find that the slope of the best fit line is 0.032. This suggests that in tropical climates, chemical weathering may account for up to 20% of the total denudation. However, silicate weathering does not account for a great portion of it. In our data, that portion is roughly 12%.

Von Blanckenburg and others (2004) observed that while erosion rates in Sri Lanka are low, so are silicate weathering rates. They attributed the low rate of silicate weathering to slow rates of physical erosion, thereby limiting the supply of readily weathered material. However, they concluded that silicate weathering represents a significant fraction of the total denudation. They found that denudation rates ranged between 5 and 30 t km^{-2} yr^{-1}, and silicate weathering ranged between 5 and 20 t km^{-2} yr^{-1}. In Panama, silicate weathering accounts for roughly 2-18% of the total denudation (Table 5.1).

West (2005) compiled previously published data on chemical weathering and physical denudation for study sites across the world. Chemical weathering rates had been determined via surface water chemistry and physical erosion using sediment fluxes or cosmogenic nuclides. After comparing both datasets, he found that in a transport-limited environment (that is, when the physical erosion is slow and limits the movement of chemically weathered material) total denudation rate – chemical and physical- explains 94% of the variability in silicate denudation rate.

Spatial scale of analysis

Both alone and together, none of the 45 landscape-scale metrics explained well the spatial variation in Panamanian basin-scale erosion rates. Although some relationships were statistically significant, there was large scatter (low R^2). When data were lumped at a regional scale, the strength of the relationships (R^2) increased, but the

statistical significance decreased (small *n*). A similar trend of weakening relationship as the analysis scale increased was found by Portenga and Bierman (2011).

No relationship was found between watershed area and erosion rate. The lack of such relationship suggests that the sediment-delivery ratio proposed by Trimble (1977) does not affect erosion rates inferred from ^{10}Be concentrations in Panamanian sediment.

Because the cosmogenic nuclide method measures the concentration of ^{10}Be, one can test effective sediment mixing within the watershed. A t-test comparing watersheds smaller than 100km^2 with those greater than 100km^2 showed that there is no significant difference in their average erosion rate ($t=-1.308$; $p = 0.306$). This lack of difference confirms that the mixing is effective and that the erosion rate of small watersheds is on average no different than that of large watersheds. Portenga and Bierman (2011) also found no relationship between erosion rates and basin area.

Tectonics and seismicity

Of the seismicity proxies analyzed, several showed a significant relationship to erosion rates. The strongest relationships with erosion rates, all negative, are the following: average magnitude of seismic events within a 75-km buffer of each watershed ($R^2 = 0.550$, $p = 0.000$), average depth of seismic events at a 50-km buffer ($R^2 = 0.466$, $p = 0.002$), average magnitude of the events at the 25-km buffer ($R^2 = 0.431$, $p = 0.005$), and average magnitude of seismic events at the 100-km buffer ($R^2 = 0.352$, $p = 0.026$). Average magnitude of the seismic events is inversely related to erosion at a variety of buffer distances.

Quantity of seismic events at the 10-km buffer (R^2 = 0.338, p = 0.033) was positively related to erosion rates (see Table 4.6). When analyzing at the regional scale, the only significant relationship (of all metrics) is held between the amount of seismic events at the 10-km buffer and erosion (R^2= 0.813, p = 0.036). This relationship is positive.

At the medium and large scale, the energy released during seismic events is the important factor, at the medium scale, it is the depth of the events and at a shorter scale, it is the number of seismic events, regardless of magnitude or depth. In the immediate scale (100m) none of the seismic variables is significantly related to erosion rates. Western Panama has the greatest density of seismic events of the country (Figure 5.2). However, the events of greater magnitude occur outside of this region. This may explain the negative relation of erosion with average magnitude of seismic events. Peak Ground Acceleration, another seismicity proxy, showed a weak positive relationship with erosion rates (R^2= 0.096, p = 0.054).

The density of seismic events is highest where some of the most rapidly eroding watersheds are located (southwestern region). The watershed for the Rio Felix (FELIX), which has the highest erosion rate (598 m/Myr), can also be related to seismic activity (see Figure 5.2). The Rio Felix is located east of the region with a high frequency of seismic events.

There is a spatial gap between the southwestern region clustering and the central one where no erosion rates were determined. A total of 10 samples were taken from this

area, but due to their low quartz content, no ^{10}Be analysis was done. Covering this spatial gap would be helpful in identifying trends in erosion rates in that region. Because of this, it is difficult to reach any specific conclusions from our data regarding the high erosion rate of Rio Felix and its relationship to seismic activity.

One of the mechanisms by which erosion may be triggered due to seismicity is by increasing landslide events. Recently, Ouimet (2008) studied the effect of M 7.9 earthquake on erosion in China. As a result of the ground shaking associated with the earthquake, slope stability was decreased. He concluded that the frequency of landslides increased erosion rates after the earthquake.

In a study examining weathering and denudation in Sri Lanka, von Blanckenburg et al. (2004) concluded that weathering and erosion were sensitive to base-level change resulting from tectonic forcing but were not accelerated by increased precipitation and temperature.

Kong et al. (2007) observed the effect of climate and tectonics on long-term erosion rates in Tibet. They concluded that there is a positive relationship between erosion and tectonics, after observing that erosion rates were similar to those in a different climate regime. They attributed this influence to the rock uplift induced by tectonics in the region. In a study of the coupling of tectonics and erosion in the Western Alps, Malusá and Vezzoli (2006) concluded that regardless of the lithology of the source area, most of the sediments produced in the region are due to tectonically-related uplift.

Erosion may also be related to uplift in Panama. Davidson (2010) measured uplift rates in the Burica Peninsula, on the border of Panama and Costa Rica, using GPS measurements. He concluded that the Burica Peninsula is uplifted at a rate of ~55mm/yr. The southwestern region we demarcated has the highest erosion rates in Panama and is located in the Burica Peninsula. Although average erosion rates are 100 times less than uplift rates, rapid uplift in this area suggests that increased denudation may be related to tectonic uplift.

It is important to point out that the response to seismic events may be tied to lithological differences. This is hard to assess in Panama, where knowledge of the geology, hidden as it is under deep jungle cover, is scarce, and the available digital information on surface geology and bedrock is not well detailed.

Topographic controls

Topographic variables (i.e. basin area, relief, slope, elevation) have been related to erosion rates in many studies (see Summerfield and Huton, 1994; Milliman and Syvitski, 1992). Erosion rates of Panamanian watersheds does not appear to be related to elevation (R^2= 0.002, p = 0.804), relief (R^2= 0.038, p = 0.232) or slope (R^2= 0.000, p = 0.951). Stepwise regressions showed no relation between erosion rates and topographic variables. This means that no combination of topographic variables or combination of a topographic and climatic (or other type of) variable is significantly related to erosion.

This findings contrast with previously published work that concluded such relationship exists. Summerfield and Huton (1994) concluded that there is a strong

relationship between relief and mechanical denudation rate. Local relief and runoff were the dominant controls on erosion in the large basins they analyzed. Milliman and Syvitski (1992) concluded from their data that basin size and topography are important controls of the export of sediment (sediment yield).

Riebe et al. (2000) used cosmogenic nuclides to measure erosion rates in seven topographically different watersheds in Sierra Nevada, California. They argued that a lack of relationship between topography and erosion rates may be indicative of equilibrium. When local base-level lowering rates are variable, erosion rates are related to average basin slope. On the other hand, if the base-level lowering rates are uniform, hillslopes exerts no control on erosion, it is rather due to bedrock erodibility. This is a potential explanation for the lack of such relationships in Panama.

Climatic control

It has been thought that both the average precipitation and exceptional hydrologic events are positively related to erosion rates (Milliman & Syvitski, 1992). However, for this research, 19 bioclimatic variables were considered, including maximum and minimum precipitation for each watershed, and none had a statistically significant relation to erosion. Mean annual precipitation exerts only a weak control in erosion at the basin scale. (R^2= 0.095, p = 0.057). When regional analysis was performed, this relationship got weaker. Temperature did not have significant relationship with erosion either at the basin (R^2= 0.002, p = 0.807) or the regional scale (R^2= 0.016, p = 0.841).

Riebe et al. (2001) concluded that climate exerted a minimal control on erosion in 7 watersheds in Sierra Nevada, California. These watersheds varied in average temperature and precipitation regime; none of these seemed to relate to erosion rates. From their research in Sri Lanka, von Blanckenburg et al. (2004) suggested that increasing temperature alone does not accelerate erosion rates. Findings of this research agree to the conclusions reached in both works.

Lithology

Analysis of Variance found no significant difference between the three geology classifications considered (igneous intrusive, volcanic, and sedimentary rocks) and erosion rates at the 0.05 significance level ($F=2.469$; $p= 0.099$). The watersheds in the southwestern region, the fastest eroding, coincide with sedimentary lithologies cropping out at the surface, a finding made world-wide by Portenga and Bierman (2011). This is also the area where the seismic activity is greater; this may imply a relationship between seismicity and the existence of sedimentary basins. However, the relationship between sedimentary lithology and higher erosion rates is significant only at the $p <0.1$.

Grain size and isotopic concentration

My data suggest that sediment introduced to Panamanian rivers by landslides has lower ^{10}Be concentrations than sediment entering the rivers by other means such as bank collapse and creep down slopes. Furthermore, the ^{10}Be concentration of the landslide material is related to grain size with large grains having 3.5 times less ^{10}Be than small grains.

The difference in isotopic concentration among grain sizes is useful to infer material sourcing. Samples with the greatest diameter result from deep-seated landslides, and carry less ^{10}Be than surface materials. Bedrock landslides can carve deeper than the attenuation length of secondary cosmic rays, bringing to the surface material that has considerably lower, if any, ^{10}Be content (Niemi et al., 2005). On the other hand, fine-grained material is preferentially sourced from near the land surface, and thus its isotopic concentration is greater.

This relationship was also found in Puerto Rico by Brown et al. (1998). In a study of chemical and physical erosion in Puerto Rico, Riebe and others (2003) observed that ^{10}Be concentrations decrease with increasing fractions of coarse material for stream sediments. They attributed this to material sourcing, and suggested that coarse fractions in stream sediments are derived from deep landslides. Given that Puerto Rico and Panama are similar in climate, it is possible that this inverse relationship between ^{10}Be concentration and grainsize will be only seen in these environments.

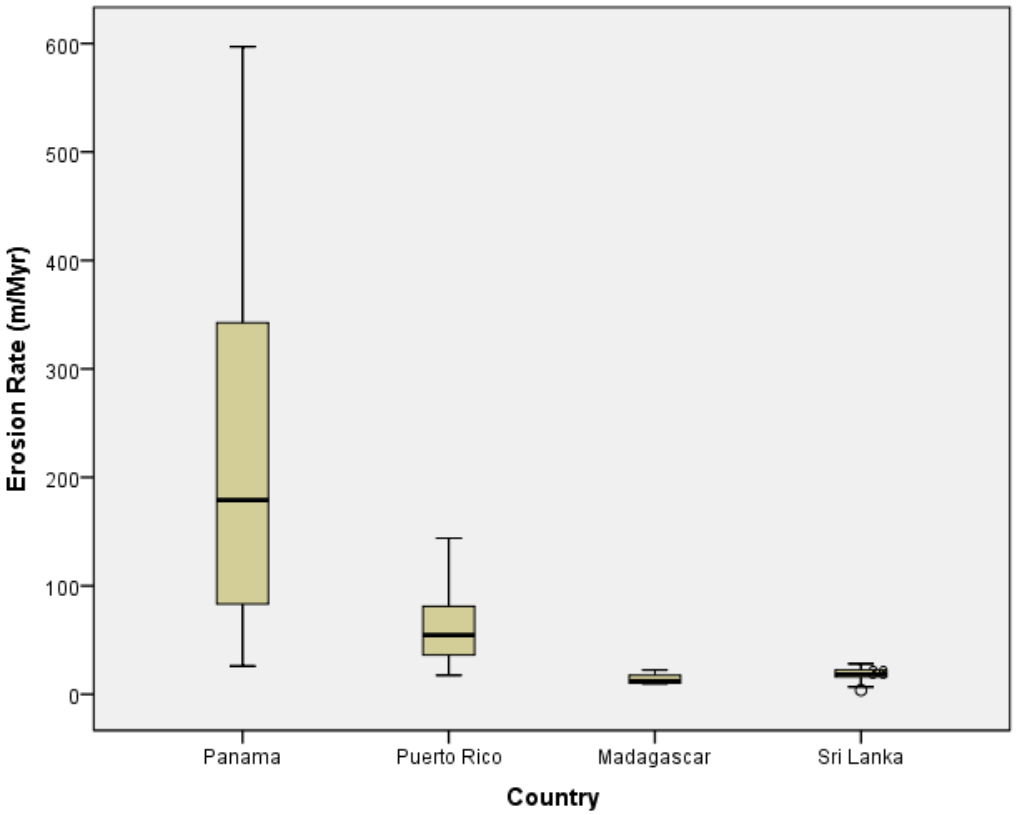

Figure 5.1: Comparison of cosmogenic-determined erosion rates in tropical climates. Lines represent the median erosion rate of published data for each country. The minimum and maximum erosion rates are represented by the horizontal lines in the bars. In Panama, erosion rates averaged 218 m/Myr (n=40), in Puerto Rico averaged 60.9 m/Myr (n=24). Erosion rate averaged 18.1 m/Myr in the 4 watersheds studied in Madagascar, and 13.9 m/Myr in Sri Lanka (n=16). Panama data previously published by Nichols et al. (2005) is not included in this figure; it will be used for spatial and temporal replicates analyses only.

Table 5.1: Silicate weathering and sediment yield in selected watersheds

River (sample ID)	Silicate weathering[1] ($t\ km^{-2}\ yr^{-1}$)	Sediment yield ($t\ km^{-2}\ yr^{-1}$)	Percent of Silicate in sediment yield
Anton (ANT)	38.6	473.6	8.2
Chagres (CHAG2009)	20.8	163.7	12.7
Chiriqui Viejo (CHVIEH)	42.7	765.6	5.6
Chico (C-NATA)	13.8	73.9	18.7
Cobre (COBRE)	26.2	204.7	12.8
Felix (FELIX)	34.2	1613.2	2.1
San Pablo (SANPAB)	26.9	361.5	7.4
Tabasara (TABA)	23.7	211.3	11.2
Vigui (VIGUI)	26.5	238.5	11.1

Comparison of sediment yield and silicate weathering rates in Panama. Silicate weathering was measured by Steven Goldsmith and Russell Harmon (unpublished data)

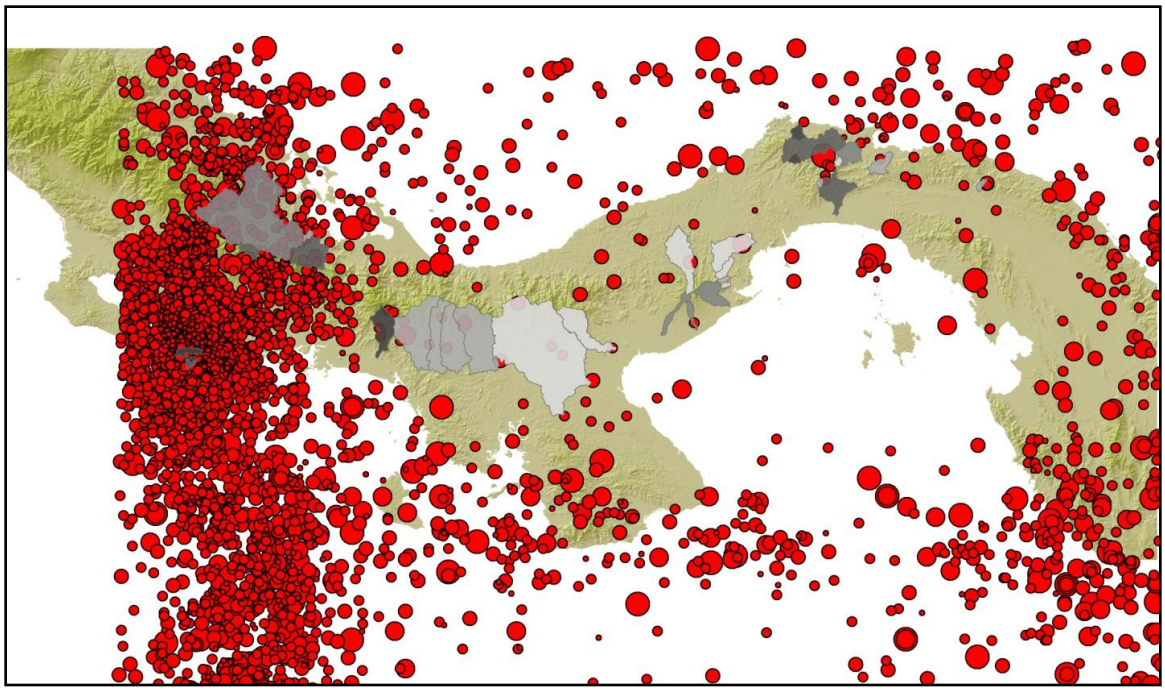

Figure 5.2: Seismic activity in Panama. Circles represent individual seismic events (1900-2011). Circle size is representative of the event magnitude. Watershed color is representative of erosion rate. Data provided by the Instituto de Geociencias (personal communication).

Chapter 6- Conclusion

This work presented the first determination of long-term erosion rates in Panama, at the country scale, using cosmogenic nuclides. They range from 26.1 m/Myr to 597 m/Myr. The great variability in erosion and its lack of relationship to topography suggests a complexity in erosive dynamics that is not possible to explain with the metrics we considered.

Based on their sediment yield calculations, Nichols et al. (2005) estimated that the main reservoir supplying water to the Panama Canal would decrease its capacity by 69% in 600 years. Our data was not compared to theirs, because some of our watersheds contain a section, but not the entire watershed they delineated. If this is not addressed correctly, comparisons are invalid. Future work includes addressing for this discrepancy in watershed overlap, in order to compare our results to Nichols et al. (2005). This will allow us to explore any changes in reservoir storage capacity based on our erosion rates.

After reviewing Panamanian government references for my work, it became evident that erosion is considered a major threat for agriculture. The percentage of terrain suitable for agriculture is small in Panama, and the devastating effects of erosion associated to it are among the main concerns for the Autoridad Nacional del Ambiente (National Environment Authority). Initiatives on sustainable forestry and agriculture have been established to try and tackle the effects of erosion (ANAM, 2008). However, there is no data about modern sediment yields for Panama in any of the government reports or scientific literature revised for this work.

Rather than extending the metrics compared to erosion, future work should be directed to filling the gaps in my work. Sampling areas where no isotopic measurements were done will potentially shed some light over erosion dynamics. This would lead to robust observations on the spatial distribution of the erosion rates in Panama.

Collecting water samples during field sampling events will help our understanding of chemical weathering rates and its relation to physical erosion. Analyzing dissolved loads in these samples will shed some light over which minerals are easily dissolved in tropical climates. This may have an effect on quartz enrichment, and therefore on the application of cosmogenic nuclides.

It would be useful to constrain modern erosion rates in the watersheds we studied. This will help assess both the change in erosion rates and the difference, if any, on the control exerted by environmental variables over different time scales (i.e. tree cover). To the best of my knowledge no information on suspended sediments data is available publicly from the Panamanian government, or recent scientific literature.

References

Adamek, S., C. Frolich, and W. Pennington. "Seismicity of Te Carubbean-Nazca Boundary: Constraints on Microplate Tectonics of the Panama Region." *Journal of Geophysical Research* 93 (1988): 2053-75.

Ahnert, F. "Functional Relationships between Denudation, Relief and Uplift in Large Mid-Latitude Drainage Basins." *American Journal of Science* 268 (1970): 243-63.

Bierman, P.R., and Kyle Keedy Nichols. "Rock to Sediment—Slope to Sea With10be—Rates of Landscape Change." *Annual Review of Earth and Planetary Sciences* 32, no. 1 (2004): 215-55.

Bierman, Paul R., Joanna M. Reuter, Milan Pavich, Allen C. Gellis, Marc W. Caffee, and Jennifer Larsen. "Using Cosmogenic Nuclides to Contrast Rates of Erosion and Sediment Yield in a Semi-Arid, Arroyo-Dominated Landscape, Rio Puerco Basin, New Mexico." *Earth Surface Processes and Landforms* 30, no. 8 (2005): 935-53.

Bierman, P. R., and Eric J. Steig. "Estimating Rates of Denudation Using Cosmogenic Isotope Abundances in Sediment." *Earth Surface Processes and Landforms* 21 (1996): 125-39.

Bilotta, G. S., and R. E. Brazier. "Understanding the Influence of Suspended Solids on Water Quality and Aquatic Biota." [In eng]. *Water Res* 42, no. 12 (Jun 2008): 2849-61.

Brown, Erik T., Robert F. Stallard, Matthew C. Larsen, Didier Bourles, L., Grant M. Raisbeck, and Francoise Yiou. "Determinarion of Predevelopment Denudation Rates of an Agricultral Watershed (Cayaguás River, Puerto Rico) Using in-Situ Produced ^{10}be in River-Borne Quartz." *Earth and Planetary Science Letters* 160 (1998): 723-28.

Brown, Erik T., Robert F. Stallard, Matthew C. Larsen, Grant M. Raisbeck, and Francoise Yiou. "Denudation Rates Determined from the Accumulation of in-Situ Produced ^{10}be in the Luquillo Experimental Forest, Puerto Rico." *Earth and Planetary Science Letters* 129 (1995): 193-202.

Bullard, W.E. "Effects of Land Use on Water Resources." *Journal of Water Pollution Control Federation* 38, no. 4 (1966): 645-59.

Camacho, E., C. Lindholm, A. Dahle, and H. Bungum. "Seismic Hazard Assessment in Panama." *Engineering Geology* 48 (1997): 1-6.

Chao, Xiaobo, Yafei Jia, F. Douglas Shields, Sam S. Y. Wang, and Charles M. Cooper. "Numerical Modeling of Water Quality and Sediment Related Processes." *Ecological Modelling* 201, no. 3-4 (2007): 385-97.

Christiansson, C. "Imagi Dam: A Study of Soil Erosion, Reservoir Sedimentation and Water Supply at Dodoma, Central Tanzani." *Geografiska Annaler, Series A, Physical Geography* 61, no. 3/4 (1979): 113-45.

Costa, John E. "Effects of Agriculture on Erosion and Sedimentation in the Piedmont Province, Maryland." *Geological Society of America Bulletin* 86 (1975): 1281-86.

Cox, Rónadh, Paul Bierman, Matthew C Jungers, and A. F Michel Rakotondrazafy. "Erosion Rates and Sediment Sources in Madagascar Inferred From10be Analysis of Lavaka, Slope, and River Sediment." *The Journal of Geology* 117, no. 4 (2009): 363-76.

Davidson, D. "Recent Uplift of the Burica Peninsula, Panama and Costa Rica, Recorded by Marine Terraces." Honors Thesis, Trinity University 2010.

Dedkov, A.P., and V.I. Moszherin. "Erosion and Sediment Yield in Mountain Regions of the World." Paper presented at the Erosion, Debris Flows and Environment in Mountain Regions, Chengdu, 1992.

Diana, M., J. D. Allan, and Infante. D. "The Influence of Physical Habitat and Land Use on Stream Fish Assemblages in Southeastern Michigan." *American Fisheries Society Symposium* 48 (2006): 359-74.

Díaz, M. Francisca, Seth Bigelow, and Juan J. Armesto. "Alteration of the Hydrologic Cycle Due to Forest Clearing and Its Consequences for Rainforest Succession." *Forest Ecology and Management* 244, no. 1-3 (2007): 32-40.

Dixon, R.K., S. Brown, R.A. Houghton, A.M. Solomon, M.C. Trexler, and J. Wisniewski. "Carbon Pools and Flux of Global Forest Ecosystems." *Science* 263, no. 5144 (1994): 185-90.

Douglas, I. "The Efficienty of Humid Tropical Denudation Systems." *Transactions of the Institute of British Geographers* 46 (1969): 1-16.

Ebbert, J. C., and R. D. Roe. "Soil Erosion in the Palouse River Basin: Indications of Improvement." edited by U.S. Geological Survey and U.S. Department of Agriculture: USGS, 1998.

El-Swaify, S. A., E. W. Dangler, and C. L. Armstrong. "Soil Erosion by Water in the Tropics." In *Research Extension Series*, 173. Honolulu, HI: University of Hawaii, 1982.

Escalante, G. "The Geology of Southern Central America and Western Colombia." Chap. 8 In *The Caribbean Region*, edited by G. Dengo and J. E. Case. The Geology of North America, 528. Boulder, CO: The Geological Society of America, 1990.

Foley, J. A., R. Defries, G. P. Asner, C. Barford, G. Bonan, S. R. Carpenter, F. S. Chapin, *et al.* "Global Consequences of Land Use." [In eng]. *Science* 309, no. 5734 (Jul 22 2005): 570-4.

García-Ruiz, J. M. "The Effects of Land Uses on Soil Erosion in Spain: A Review." *Catena* 81, no. 1 (2010): 1-11.

Gosse, John C., and Fred M. Phillips. "Terrestrial in Situ Cosmogenic Nuclides: Theory and Application." *Quaternary Science Reviews* 20 (2001): 1475-560.

Granger, Darryl E., James W. Kirchner, and R. C. Finkel. "Spatially Averaged Long-Term Erosion Rates Measured from in-Situ Produced Cosmogenic Nuclides in Alluvial Sediment." *The Journal of Geology* 104 (1996): 249-57.

Harden, Carol P. "Human Impacts on Headwater Fluvial Systems in the Northern and Central Andes." *Geomorphology* 79, no. 3-4 (2006): 249-63.

Harmon, R. S. "Geological Development of Panama." In *The Río Chagres, Panama: A Multidisciplinary Profile of a Tropical Watershed*, edited by R. S. Harmon. 354. Netherlands: Springer, 2005.

Haruna, A. "Measuring Protected Areas' Impact on Deforestation in Panama." Duke University, 2010.

Hewawasam, Tilak, Friedhelm von Blanckenburg, M. Schaller, and Peter Kubik. "Increase of Human over Natural Erosion Rates in Tropical Highlands Constrined by Cosmogenic Nuclides." *Geology* 31, no. 7 (2003): 597-600.

Hooke, R.L. "On the Efficacy of the Humans as Geomorphic Agents." *GSA Today* 4, no. 9 (1994): 217, 24-25.

Hooke, R.L.. "On the History of Humans as Geomorphic Agents." *Geology* 28, no. 9 (2000): 843-46.

Hunt, A. L., G. A. Petrucci, P. R. Bierman, and R. C. Finkel. "Metal Matrices to Optimize Ion Beam Currents for Accelerator Mass Spectrometry." *Nuclear Instruments and Methods in Physics Research Section B: Beam Interactions with Materials and Atoms* 243, no. 1 (2006): 216-22.

Judson, S. "Erosion of the Land, or What's Happening to Our Continents?". *American Scientist* 56, no. 4 (1968): 356-74.
Kellogg, J.N., and V. Vega. "Tectonic Development of Panama, Costa Rica, and the Colombian Andes: Constraints from Global Positioning System Geodetic Studies and Gravity." *Geological Society of America* Special Paper 295 (1995): 75-90.
Kohl, C. P., and K. Nishiizumi. "Chemical Isolation of Quartz for Measurement of in-Situ Produced Cosmogenic Nuclides." *Geochimica et Cosmochimica Acta* 56 (1992): 3583-87.
Kong, Ping, Chunguang Na, David Fink, Lin Ding, and Feixin Huang. "Erosion in Northwest Tibet Fromin-Situ-Produced Cosmogenic10be And26al in Bedrock." *Earth Surface Processes and Landforms* 32, no. 1 (2007): 116-25.
Lal, D., and J.R. Arnold. "Tracing Quartz through the Environment." *Proceedings of the Indian Academic of Science (Earth and Planetary Science)* 94 (1985): 1-5.
Lal, D., and B Peters. "Cosmic-Ray Produced Radioactivity on the Earth." In *Handuch Der Physik*, edited by K. Sitte. 551-612. New York: Springer-Verlag, 1967.
Lewis, J. "Evaluating the Impacts of Logging Activities on Erosion and Suspended Sediment Transport in the Caspar Creek Watersheds." USDA- Forest Service, 1998.
Malusà, Marco G., and Giovanni Vezzoli. "Interplay between Erosion and Tectonics in the Western Alps." *Terra Nova* 18, no. 2 (2006): 104-08.
Marsh, G. P. *Man and Nature, or Physical Geography as Modified by Human Action*. New York: Scribners, 1864.
Marshall, E., and J. Shortle. "Urban Development Impacts on Ecosystems." In *Land Use Problems and Conflicts: Causes, Consequences and Solution*, edited by S. Goetz, S. Shortle and J. Bergstrom. 61-72. New York: Routledge Publishing, 2005.
Massoudieh, A., F. A. Bombardelli, and T. R. Ginn. "A Biogeochemical Model of Contaminant Fate and Transport in River Waters and Sediments." [In eng]. *J Contam Hydrol* 112, no. 1-4 (Mar 1 2010): 103-17.
Matson, P.A., W.J. Parton, A.G. Power, and M.J. Swift. "Agricultural Intensification and Ecosystem Properties." *Science* 277, no. 5325 (1997): 504-09.
Menard, H.W. . "Some Rates of Regional Erosion." *The Journal of Geology* 69, no. 2 (1961): 154-61.
Milliman, J. D., and J. P. Syvitski. "Geomorphic/Tectonic Control of Sediment Discharge to the Ocean: The Importance of Small Mountainous Rivers." *The Journal of Geology* 100 (1992): 525-44.
Mohammad, Ayed G., and Mohammad A. Adam. "The Impact of Vegetative Cover Type on Runoff and Soil Erosion under Different Land Uses." *Catena* 81, no. 2 (2010): 97-103.
Montgomery, D. R. "Soil Erosion and Agricultural Sustainability." [In eng]. *Proc Natl Acad Sci U S A* 104, no. 33 (Aug 14 2007): 13268-72.
Nichols, Kyle K., Paul R. Bierman, Robert Finkel, and Jennifer Larsen. "Long-Term (10 to 20 Kyr) Sediment Generation Rates for the Upper Rio Chagres Basin Based on Cosmogenic ^{10}be." In *The Rio Chagres, Panama: A Multidisciplinary Profile of a Tropical Watershed*, edited by Russell S. Harmon. 354. The Netherlands: Springer, 2004.
Niemi, Nathan A., Michael Oskin, Douglas W. Burbank, Arjun M. Heimsath, and Emmanuel J. Gabet. "Effects of Bedrock Landslides on Cosmogenically Determined Erosion Rates." *Earth and Planetary Science Letters* 237, no. 3-4 (2005): 480-98.
Nishiizumi, K., D. Lal, J. Klein, R. Middleton, and J.R. Arnold. "Production of ^{10}be and ^{26}al by Cosmic Rays in Terrestrial Quartz in Situ and Implications for Erosion Rates." *Nature* 319 (1986): 134-36.

Norton, M. M., and T.R. Fisher. "The Effects of Forest on Stream Water Quality in Two Coastan Plain Watersheds of the Chesapeake Bay." *Ecological Engineering* 14 (2000): 337-62.
Ouimet, William B. "Landslides Associated with the May 12, 2008 Wenchuan Earthquake: Implications for the Erosion and Tectonic Evolution of the Longmen Shan." *Tectonophysics* 491, no. 1-4 (2010): 244-52.
Ouyang, W., A. K. Skidmore, F. Hao, and T. Wang. "Soil Erosion Dynamics Response to Landscape Pattern." [In eng]. *Sci Total Environ* 408, no. 6 (Feb 15 2010): 1358-66.
Palka, E. J. "A Geographic Overview of Panama." In *The Rio Chagres, Panama. A Multidisciplinary Profile to a Tropical Watershed*, edited by Russell S. Harmon. 3-18. Netherlands: Springer, 2005.
Palumbo, L., R. Hetzel, M. Tao, and X. Li. "Topographic and Lithologic Control on Catchment-Wide Denudation Rates Derived from Cosmogenic ^{10}be in Two Mountain Ranges at the Margin of Ne Tibet." *Geomorphology* 117, no. 1-2 (2010): 130-42.
Panamá, Contraloría General de la República de. "Estadísticas Ambientales: Años 2000-04." edited by Instituto Nacional de Estadística y Censo. Panamá, República de Panamá: Contraloría General de la República de Panamá, 2005.
Panamá, Contraloría General de la República de. "Estadísticas Ambientales: Años 2000-2004." Instituto Nacional de Estadística y Censo, 2008.
Panamá, Contraloría General de la República de. "Informe Final De Resultados De Cobertura Boscosa Y Uso Del Suelo En La República De Panamá:1992-2000." edited by Autoridad Nacional del Ambiente- ANAM, 2003.
Panamá, Contraloría General de la República de. "Plan Nacional de Desarrollo Forestal: Modelo Forestal Sostenible." edited by Autoridad Nacional del Ambiente- ANAM, 2008.
Pimentel, D., C. Harvey, P. Resosudarmo, K. Sinclair, D. Kurz, M. McNair, S. Crist, *et al.* "Environmental and Economic Costs of Soil Erosion and Conservation Benefits." *Science* 267, no. 5201 (1995): 1117-23.
Portenga, Eric W., and Paul R. Bierman. "Understanding Earth's Eroding Surface with ^{10}be." *GSA Today* 21, no. 8 (2011): 4-10.
Ramírez, C.A. "Estado De La Diversidad Biológica De Los Árboles Y Bosques De Panamá." Roma, Italia: FAO, 2003.
Ramos-Scharron, C. E., and L. H. Macdonald. "Development and Application of a Gis-Based Sediment Budget Model." [In eng]. *J Environ Manage* 84, no. 2 (Jul 2007): 157-72.
Randhir, Timothy O., and Ashley G. Hawes. "Watershed Land Use and Aquatic Ecosystem Response: Ecohydrologic Approach to Conservation Policy." *Journal of Hydrology* 364, no. 1-2 (2009): 182-99.
Riebe, Clifford S., James W. Kirchner, and Robert C. Finkel. "Erosional and Climatic Effects on Long-Term Chemical Weathering Rates in Granitic Landscapes Spanning Diverse Climate Regimes." *Earth and Planetary Science Letters* 224, no. 3-4 (2004): 547-62.
Riebe, Clifford S., James W. Kirchner, and Robert C. Finkel. "Long-Term Rates of Chemical Weathering and Physical Erosion from Cosmogenic Nuclides and Geochemical Mass Balance." *Geochimica et Cosmochimica Acta* 67, no. 22 (2003): 4411-27.
Riebe, Clifford S., James W. Kirchner, and Darryl E. Granger. "Quantifying Quartz Enrichment and Its Consequences for Cosmogenic Measurements of Erosion Rates from Alluvial Sediment and Regolith." *Geomorphology* 40 (2001): 15-19.
Riebe, Clifford S., James W. Kirchner, Darryl E. Granger, and Robert Finkel. "Erosional Equilibrium and Disequilibrium in the Sierra Nevada, Inferred from Cosmogenic ^{26}al and ^{10}be in Alluvial Sediment." *Geology* 28, no. 9 (2000): 803-06.

Riebe, C. S., J. W. Kirchner, D. E. Granger, and R. C. Finkel. "Erosional Equilibrium and Disequilibrium in the Sierra Nevada, Inferred from Cosmogenic ^{26}al and ^{10}be in Alluvial Sediment." *Geology* 28, no. 9 (2000): 803-06.

Riebe, Clifford S., James W. Kirchner, Darryl E. Granger, and R. C. Finkel. "Minimal Climatic Control on Erosion Rates in the Sierra Nevada, California." *Geology* 29, no. 5 (2001): 447-50.

Ritter, D. F., R. C. Kochel, and J. R. Miller. *Process Geomorphology* 3rd ed. Dubuque, IA: W.C. Brown Publishers, 1995.

Rochibaud, P.R. "Measurement of Post-Fire Hillslope Erosion to Evaluate and Model Rehabilitation Treatment Effectiveness and Recovery." *International Journal of Wildland Fire* 14 (2005): 574-485.

Ryan, P. A. "Environmental Effects of Sediment on New Zealand Streams: A Review." *New Zealand Journal of Marine and Freshwater Research* 25 (1991): 207-21.

Schuchert, C. "Panama." Chap. 37 In *Historical Geology of the Antillean-Caribbean Region or the Lands Bordering the Gulf of Mexico and the Caribbean Sea*. 810. New York: John Wiley & Sons, 1995.

Sirvent, J., G. Desir, M. Gutierrez, C. Sancho, and G. Benito. "Erosion Rates in Badland Areas Recorded by Collectors, Erosion Pins and Profilometer Techniques (Ebro Basin, Ne-Spain)." *Geomorphology* 19 (1997): 61-75.

Soulsby, C., A. F. Youngson, H. J. Hoir, and I. A. Malcolm. "Fine Sediment Influence on Salmonid Spawning Habitat in a Lowland Agricultural Stream: A Preliminary Assessment." *The Science of the Total Environment* 265 (2001): 295-307.

Sthiannopkao, S., S. Takizawa, J. Homewong, and W. Wirojanagud. "Soil Erosion and Its Impacts on Water Treatment in the Northeastern Provinces of Thailand." [In eng]. *Environ Int* 33, no. 5 (Jul 2007): 706-11.

Stroosnijder, Leo. "Measurement of Erosion: Is It Possible?". *Catena* 64, no. 2-3 (2005): 162-73.

Summerfield, M. A. *Global Geomorphology: An Introduction to the Study of Landforms*. New York, USA: John Wiley & Sons, 1991.

Summerfield, M. A., and N. J. Hulton. "Natural Controls of Fluvial Denudation Rates in Major World Drainage Basins." *Journal of Geophysical Research* 99, no. B7 (1994): 13871-83.

Syvitski, J. P., C. J. Vorosmarty, A. J. Kettner, and P. Green. "Impact of Humans on the Flux of Terrestrial Sediment to the Global Coastal Ocean." [In eng]. *Science* 308, no. 5720 (Apr 15 2005): 376-80.

Terry, R. A. *A Geological Reconnaissance of Panama*. San Francisco, CA: California Academy of Sciences, 1956.

Thoma, David P., Satish C. Gupta, Marvin E. Bauer, and C. E. Kirchoff. "Airborne Laser Scanning for Riverbank Erosion Assessment." *Remote Sensing of Environment* 95, no. 4 (2005): 493-501.

Tong, S. T. Y., and W. Chen. "Modeling the Relationship between Land Use and Surface Water Quality." *Journal of Envionmental Management* 66 (2002): 377-93.

Trimble, S.W. "Contribution of Stream Channel Erosion to Sediment Yield from an Urbanizing Watershed." *Science* 278 (1997): 1442-44.

Trimble, S.W.. "The Fallacy of Stream Equilibrium in Contemporary Denudation Studies." *American Journal of Science* 277 (1977): 876-87.

Tuniz, C., J. R. Bird, D. Fink, and G. F. Herzog. *Accelerator Mass Spectrometry: Ultrasensitive Analysis for Global Science*. CRC Press, 1998.

U. S. Environmental Protection Agency. "Stressor Identification Guidance Document." edited by USEPA, 228. Washington, D. C., 2000.

Vanacker, Veerle, Gerard Govers, Sanddra Barros, Jean Poesen, and Jozef Deckers. "The Effect of Short-Term Socio-Economic and Demographic Change on Landuse Dynamics and Its Corresponding Geomorphic Response with Relation to Water Erosion in a Tropical Mountainous Catchment, Ecuador." *Landscape Ecology* 18 (2003): 1-15.

Vanacker, Veerle, Friedhelm von Blanckenburg, Gerard Govers, Armando Molina, Jean Poesen, Jozef Deckers, and Peter Kubik. "Restoring Dense Vegetation Can Slow Mountain Erosion to near Natural Benchmark Levels." *Geology* 35, no. 4 (2007): 303-06.

Varela, Sara, Jesús Rodríguez, and Jorge M. Lobo. "Is Current Climatic Equilibrium a Guarantee for the Transferability of Distribution Model Predictions? A Case Study of the Spotted Hyena." *Journal of Biogeography* 36, no. 9 (2009): 1645-55.

Vitousek, P.M., H.A. Mooney, J. Lubchenco, and J.M. Melillo. "Human Domination of Earth's Ecosystems." *Science* 277 (1997): 494-99.

von Blanckenburg, Friedhelm. "The Control Mechanisms of Erosion and Weathering at Basin Scale from Cosmogenic Nuclides in River Sediment." *Earth and Planetary Science Letters* 237 (2005): 462-79.

von Blanckenburg, F., T. Hewawasam, and P.W. Kubik. "Cosmogenic Nuclide Evidence for Low Weathering and Denudation in the Wet, Tropical Highlands of Sri Lanka." *Journal of Geophysical Research* 109, no. F3 (2004).

Vrieling, Anton. "Satellite Remote Sensing for Water Erosion Assessment: A Review." *Catena* 65, no. 1 (2006): 2-18.

West, A., A. Galy, and M. Bickle. "Tectonic and Climatic Controls on Silicate Weathering." *Earth and Planetary Science Letters* 235, no. 1-2 (2005): 211-28.

Wilber, D. H., and D. G. Clarke. "Biological Effects of Suspended Sediments: A Review of Suspended Sediment Impacts on Fish and Shellfish with Relation to Dredging Activities in Estuaries." *North American Journal of Fisheries Management* 21 (2001): 855-75.

Wilkinson, Bruce H. "Humans as Geologic Agents: A Deep-Time Perspective." *Geology* 33, no. 3 (2005): 161.

Wilkinson, B. H., and B. J. McElroy. "The Impact of Humans on Continental Erosion and Sedimentation." *Geological Society of America Bulletin* 119, no. 1-2 (2007): 140-56.

Wolman, M. G. "A Cycle of Sedimentation and Erosion in Urban River Channels." *Geografiska Annaler* 49A (1967): 385-95.

Wolman, M. G., and A. P. Schick. "Effects of Construction on Fluvial Sediment, Urban and Suburban Areas of Maryland." *Water Resources Research* 3, no. 2 (1967): 451-64.

:

Appendix 1 – Data Table

SAMPLE ID	River	Region	Sample collection year	Be content (atoms/g)
ANT	Anton	Central-East	2007	22736
BART	Bartolo	Southwest	2007	7382
BLA	Boqueron- Outlet	Eastern	2004	15131
C_NATA	Chico near Nata	Central	2007	137018
CAIM	Caimito	Central-East	2007	95438
CAPI	Capira	Central-East	2007	34790
CHAG2009	Chagres Headwaters	Eastern	2009	68118
CHAME	Chame	Central-East	2007	23745
CHAN	Changuanolo	Northwest	2007	39381
CHVIE_H	Chiriqui Viejo Headwaters	Northwest	2007	36064
CNGO	Cuango	Eastern	2007	14335
COBRE	Cobre	Central	2007	51726
CORO	Corotu	Southwest	2007	7911
CUAN	Cuango	Eastern	2004	10468
CUL	Culebra	Eastern	2004	13058
DIOS	Nombre de Dios	Eastern	2007	8296
FELIX	Felix	Central	2007	7989
GLOR	La Gloria	Northwest	2007	35377
GRUMO	Guarumo	Northwest	2007	17604
GUAN	Guanabano	Southwest	2007	9782
GUI	Guias	Central-East	2007	18105
IND	Indio	Central-East	2004	66398
MAND	Mandingo	Eastern	2007	19630
MARIA	Santa Maria	Central	2007	55591
NDD	Nombre de Dios	Eastern	2004	9035
PACORA	Pacora	Eastern	2007	10874
PAN02	Carti Grande	Eastern	2007	31714
PAN06	Diablo	Eastern	2007	36071
PERE	Perequite	Central-East	2007	112422
PHW	Pequini Headwaters	Eastern	2004	10501
PLA	Pequini- Outlet	Eastern	2004	9399
PLS	Chagres	Eastern	2009	23201
PSM	Pequini	Eastern	2004	12402
ROBO	Rohalo	Northwest	2007	30529
SAJ	Sajlices	Central-East	2007	138725
SAN_T	San Cristobal	Eastern	2004	57578
SANPAB	San Pablo	Central	2007	31829
SMP	San Miguel	Eastern	2004	14486
TABA	Tabasar	Central	2007	61909
VIGUI	Vigui	Central	2007	50703

SAMPLE ID	Erosion Rate (m/Myr)	Log10_ER	Average Slope (°)	Area (km^2)
ANT	175	2.24	6.36	84.18
BART	505	2.70	7.24	61.23
BLA	258	2.41	11.6	90.06
C_NATA	27.4	1.44	10.3	343.8
CAIM	34.1	1.53	4.97	295.85
CAPI	115	2.06	14.08	19.86
CHAG2009	60.6	1.78	9.21	20.11
CHAME	168	2.23	11.04	183.16
CHAN	160	2.20	17.6	1690
CHVIE_H	284	2.45	16.45	66.77
CNGO	262	2.42	4.54	158.02
COBRE	75.8	1.88	9.16	463.09
CORO	459	2.66	7.37	13.63
CUAN	366	2.56	11.54	132.18
CUL	291	2.46	11.38	33.36
DIOS	441	2.64	8.72	53.05
FELIX	597	2.78	17.01	244.07
GLOR	124	2.09	17.12	23.49
GRUMO	283	2.45	18.24	312.72
GUAN	367	2.56	6.65	20.89
GUI	221	2.34	6.78	43.85
IND	54.1	1.73	8.28	356.54
MAND	192	2.28	10.04	136.74
MARIA	68	1.83	7.91	2410
NDD	403	2.61	8.28	58.6
PACORA	366	2.56	9.61	255.51
PAN02	116	2.06	9.49	101.6
PAN06	107	2.03	10.59	24.29
PERE	29.1	1.46	7.14	64.74
PHW	378	2.58	9.58	32.06
PLA	417	2.62	10.11	146.18
PLS	183	2.26	9.83	56.5704
PSM	319	2.50	10.49	70.76
ROBO	148	2.17	16.82	134.74
SAJ	26.1	1.42	15.37	15.01
SAN_T	76.2	1.88	14.14	15.97
SANPAB	134	2.13	10.93	690.33
SMP	268	2.43	11.02	42.8
TABA	78.2	1.89	14.15	645.37
VIGUI	88.2	1.95	12.02	310.34

SAMPLE ID	Relief (m)	Elevation (m)	Average Temperature (°C)	Mean Diurnal Range (°C)
ANT	1118	383	25.3	8.1
BART	614	171.7	25.5	10.1
BLA	896	311	24.9	6.9
C_NATA	1703	487.9	24.6	9.2
CAIM	568	151.5	26.4	7.4
CAPI	828	422.8	25.4	7.8
CHAG2009	422	562.5	23.6	7.3
CHAME	1132	389.2	25.3	7.9
CHAN	3315	1334.2	20.0	9.1
CHVIE_H	1501	2289.6	14.0	9.1
CNGO	282	220.9	26.4	6.9
COBRE	1643	426.1	24.4	9.5
CORO	245	112.4	25.7	10.0
CUAN	728	249.9	25.3	7.1
CUL	643	237.3	25.4	7.1
DIOS	440	131.8	26.0	6.7
FELIX	2287	723.7	23.0	9.3
GLOR	1436	616.8	23.3	8.7
GRUMO	2303	832.4	22.7	8.9
GUAN	230	96.7	25.7	10.0
GUI	794	372	25.4	8.1
IND	1092	284.5	25.9	7.4
MAND	712	244.2	25.4	7.3
MARIA	1818	360.2	25.1	9.8
NDD	442	124.3	26.0	6.7
PACORA	923	334.2	25.0	7.7
PAN02	552	229.4	25.5	7.4
PAN06	528	352.7	25.0	7.3
PERE	854	195.5	26.3	7.6
PHW	434	328	24.8	7.0
PLA	602	298.6	25.4	7.0
PLS	32.69	516.1	23.8	7.3
PSM	704	330.7	24.8	7.0
ROBO	1855	668.2	23.2	8.7
SAJ	944	430.3	24.9	7.9
SAN_T	680	661.4	23.1	7.4
SANPAB	1839	548.5	23.8	9.5
SMP	441	295.7	24.9	7.0
TABA	2146	860.7	22.4	9.3
VIGUI	1869	687.4	23.3	9.4

SAMPLE ID	Isothermality (%)	Temperature Seasonality (°C)	Max Temp Warmest Month (°C)	Min Temp Coldest Month (°C)
ANT	76.6	6.5	31.3	20.7
BART	74.8	6.9	32.7	19.3
BLA	70.9	7.8	30.0	20.3
C_NATA	74.7	5.7	31.4	19.2
CAIM	77.2	5.7	31.6	22.1
CAPI	77.3	5.9	30.8	20.8
CHAG2009	72.9	6.6	28.8	18.8
CHAME	77.4	6.1	31.0	20.9
CHAN	78.9	5.4	25.7	14.2
CHVIE_H	77.9	6.1	19.6	8.0
CNGO	74.0	6.5	31.3	21.9
COBRE	74.0	5.0	31.4	18.6
CORO	74.8	6.7	32.9	19.5
CUAN	72.7	6.9	30.4	20.8
CUL	73.9	6.4	30.4	20.9
DIOS	71.5	7.7	31.0	21.6
FELIX	74.7	5.1	29.7	17.3
GLOR	77.6	5.0	28.8	17.7
GRUMO	77.2	5.0	28.2	16.8
GUAN	74.7	6.6	32.9	19.6
GUI	76.9	6.5	31.4	20.9
IND	75.9	6.5	31.1	21.5
MAND	75.2	5.8	30.4	20.8
MARIA	72.8	5.4	32.3	18.9
NDD	71.3	7.7	31.0	21.6
PACORA	75.4	5.1	30.2	20.1
PAN02	77.1	5.0	30.4	20.9
PAN06	78.2	4.4	29.5	20.2
PERE	78.2	5.5	31.7	22.1
PHW	71.7	7.4	29.9	20.2
PLA	72.1	7.6	30.7	21.0
PLS	72.8	6.6	29.0	19.1
PSM	71.8	7.4	30.0	20.2
ROBO	77.9	5.1	28.7	17.5
SAJ	77.8	5.8	30.8	20.7
SAN_T	73.1	6.5	28.4	18.4
SANPAB	74.7	4.3	30.6	17.9
SMP	71.4	7.6	30.0	20.4
TABA	74.9	5.1	29.0	16.7
VIGUI	74.3	5.3	30.1	17.6

SAMPLE ID	Temp Annual Range (°C)	Mean Temp Wettest Quarter (°C)	Mean Temp Driest Quarter (°C)	Mean Temp Warm Quarter (°C)
ANT	10.6	24.8	25.7	26.4
BART	13.4	25.0	25.7	26.5
BLA	9.6	24.0	25.3	25.9
C_NATA	12.2	24.3	24.9	25.6
CAIM	9.5	25.8	26.6	27.1
CAPI	10.0	24.7	25.6	26.1
CHAG2009	9.9	23.0	23.6	24.5
CHAME	10.2	24.8	25.7	26.3
CHAN	11.5	20.0	19.6	20.6
CHVIE_H	11.6	14.4	13.4	14.7
CNGO	9.3	25.7	26.6	27.3
COBRE	12.7	24.0	24.6	25.1
CORO	13.3	25.2	25.9	26.7
CUAN	9.6	24.6	25.5	26.3
CUL	9.6	24.8	25.4	26.3
DIOS	9.4	25.1	26.7	27.1
FELIX	12.4	22.6	23.1	23.8
GLOR	11.2	23.4	23.0	24.0
GRUMO	11.4	22.5	22.2	23.1
GUAN	13.3	25.3	26.0	26.7
GUI	10.5	24.9	25.9	26.5
IND	9.6	25.2	26.0	26.8
MAND	9.6	24.8	25.3	26.2
MARIA	13.4	24.8	25.2	26.0
NDD	9.4	25.1	26.7	27.1
PACORA	10.1	24.5	25.0	25.7
PAN02	9.5	25.0	25.5	26.2
PAN06	9.3	24.6	24.8	25.4
PERE	9.7	25.8	26.7	27.1
PHW	9.7	24.0	25.4	25.8
PLA	9.7	24.8	25.5	26.6
PLS	9.9	23.2	23.9	24.7
PSM	9.7	24.1	25.2	25.9
ROBO	11.2	23.3	22.8	23.8
SAJ	10.1	24.6	25.5	26.0
SAN_T	10.1	22.7	23.2	24.1
SANPAB	12.6	23.5	23.9	24.4
SMP	9.7	24.1	25.4	25.9
TABA	12.3	22.0	22.6	23.1
VIGUI	12.6	22.9	23.6	24.1

SAMPLE ID	Mean Temp Coldest Quarter (°C)	Annual Precipitation (mm)	Precip Wettest Month (mm)	Precip Driest Month (mm)
ANT	24.7	2269.4	426.1	7.4
BART	24.7	2676.6	549.8	36.8
BLA	23.9	3142.9	462.2	53.2
C_NATA	24.2	2510	490.5	18.5
CAIM	25.7	2169.7	382.2	9.7
CAPI	24.6	2392.2	487.9	42.5
CHAG2009	22.8	3175.2	467.7	42.0
CHAME	24.8	2388.2	478.7	74.8
CHAN	19.3	2791.5	407.1	40.1
CHVIE_H	13.1	2446.8	390.1	7.9
CNGO	25.6	2737.3	397.5	31.2
COBRE	23.9	3019.9	503.2	20.2
CORO	24.9	2559.7	530.6	34.9
CUAN	24.5	2933.2	410.0	41.5
CUL	24.6	2840.2	393.9	36.6
DIOS	25.1	3053.1	457.5	43.5
FELIX	22.5	3116.5	499.7	62.8
GLOR	22.7	3360.9	437.1	130.1
GRUMO	21.9	3246.0	445.9	110
GUAN	24.9	2543.3	526.5	34
GUI	24.9	2326.9	458.7	4.7
IND	25.1	3085.8	453.8	37.8
MAND	24.7	2758.1	399.1	32.0
MARIA	24.6	2599.5	466.2	10.5
NDD	25.1	3053.9	459.4	43.4
PACORA	24.3	2712.7	466.1	19.6
PAN02	24.9	2557.7	425.2	23.0
PAN06	24.2	2218.4	353.9	28.2
PERE	25.8	2073.8	391.9	17.4
PHW	23.9	3093.3	438.6	52.1
PLA	24.6	2995.5	414.3	44.1
PLS	23.0	3136.5	448.7	43.9
PSM	23.9	3072.6	430.6	50.0
ROBO	22.5	3189.7	423.9	103.2
SAJ	24.6	2380.5	492.6	9.1
SAN_T	22.3	3338.1	555	19.0
SANPAB	23.3	2865.2	485.7	31.8
SMP	24.0	3103.4	448.5	52.7
TABA	21.8	2943.5	470.1	45.3
VIGUI	22.7	2970.4	475.7	33.6

SAMPLE ID	Precip Seasonality (mm)	Precip Wettest Quarter (mm)	Precip Driest Quarter(mm)	Precip Warmest Quarter (mm)
ANT	69.3	1021.2	48.0	336.1
BART	66.4	1221.8	126.9	425.3
BLA	48.0	1119.6	241.6	509.6
C_NATA	74.8	1202.0	49.4	348.7
CAIM	63.6	947.6	78.6	345.2
CAPI	73.1	1117.8	47.9	354.4
CHAG2009	52.2	1236.7	205.7	507.5
CHAME	73.2	1111.8	43.6	361.3
CHAN	46.3	1031.4	260.3	677.5
CHVIE_H	53.9	962.8	165.6	774.0
CNGO	51.5	1008.7	181.2	433.7
COBRE	66.9	1327.9	82.7	408.1
CORO	67.0	1173.4	117.8	398.3
CUAN	49.2	1072.8	214.0	470.1
CUL	50.6	1064.1	197.3	450.1
DIOS	49.8	1095.9	216.5	491.2
FELIX	54.4	1263.3	211.5	524.5
GLOR	34.2	1135.5	436.5	747.6
GRUMO	40.2	1154.2	380.0	715.0
GUAN	67.4	1167.6	113.3	393.7
GUI	73.0	1077.8	33.0	355.8
IND	54.0	1177.9	173.8	497.7
MAND	53.5	1073.8	169.0	435.5
MARIA	71.6	1213.4	67.1	412.2
NDD	50.0	1098.1	215.6	490.9
PACORA	63.1	1163.3	102.3	433.0
PAN02	58.7	1044.4	128.6	401.4
PAN06	58.3	904.2	114.0	343.9
PERE	66.7	928.1	67.6	297.1
PHW	46.7	1096.6	246.7	500.6
PLA	48.6	1065.2	215.1	486.3
PLS	51.4	1211.1	209.8	499.7
PSM	47.5	1097.9	237.5	498.1
ROBO	38.5	1109.5	372.8	759.5
SAJ	74.7	1123.4	44.1	329.0
SAN_T	60.2	1388.1	150.6	534.8
SANPAB	67.6	1289.0	89.9	421.6
SMP	47.2	1095.1	244.3	502.9
TABA	57.5	1211.2	161.5	500.3
VIGUI	61.3	1251.4	124.0	443.1

SAMPLE ID	Precip Coldest Quarter (mm)	Tree cover (%)	Geology	Chemical Weathering ($t\ km^{-2}yr^{-1}$)
ANT	859.4	68.2	Volcanic	38.6
BART	964.9	54.2	Sedimentary	
BLA	1013.5	74.4	Volcanic	
C_NATA	1027.6	53.4	Volcanic	13.8
CAIM	824.3	114.9	Volcanic	
CAPI	922.8	72.7	Volcanic	
CHAG2009	764.3	79.0	5	20.8
CHAME	965.4	83.3	Volcanic	
CHAN	415.8	84.8	Volcanic	
CHVIE_H	276.0	66.6	Volcanic	42.7
CNGO	837.7	64.3	Volcanic	
COBRE	1071.2	55.7	Volcanic	26.2
CORO	934.7	49.6	Sedimentary	
CUAN	922.1	79.8	Volcanic	
CUL	849.5	79.0	Volcanic	
DIOS	1001.3	68.0	Volcanic	
FELIX	762.1	63.4	Volcanic	34.2
GLOR	575.1	80.0	Volcanic	
GRUMO	525.6	92.0	Volcanic	
GUAN	932.7	59.2	Sedimentary	
GUI	932.0	36.9	Volcanic	
IND	1092.4	71.4	Volcanic	
MAND	812.7	79.0	Volcanic	
MARIA	857.4	51.7	Volcanic	
NDD	1002.5	66.9	Volcanic	
PACORA	671.8	63.9	Intrusive igneous	
PAN02	702.7	78.9	Intrusive igneous	
PAN06	504.2	79.3	Volcanic	
PERE	851.3	106.0	Volcanic	
PHW	1009.5	77.2	Volcanic	
PLA	913.9	63.1	Volcanic	
PLS	801.9	79.0	Intrusive igneous	
PSM	951.8	79.5	Volcanic	
ROBO	477.3	80.4	Volcanic	
SAJ	947.2	87.4	Volcanic	
SAN_T	662.5	80.0	Intrusive igneous	
SANPAB	923.9	62.5	Volcanic	26.9
SMP	1000.1	79.1	Volcanic	
TABA	830.9	63.9	Volcanic	23.7
VIGUI	943.5	74.5	Volcanic	26.5

SAMPLE ID	Peak Ground Acc(g)	SeismicEvts100m	AvgDepth100m (km)	AvgMag100m (Mw)
ANT	1.79	0	0.0	0.0
BART	4.36	43	14.6	4.0
BLA	1.78	0	0.0	0.0
C_NATA	1.79	1	33.0	4.4
CAIM	1.86	1	13.0	5.3
CAPI	1.83	0	0.0	0.0
CHAG2009	1.83	0	0.0	0.0
CHAME	1.82	0	0.0	0.0
CHAN	3.59	58	23.7	3.8
CHVIE_H	3.74	0	0.0	0.0
CNGO	1.8	0	0.0	0.0
COBRE	2.23	1	7.0	4.3
CORO	4.34	13	18.0	4.4
CUAN	1.8	0	0.0	0.0
CUL	1.82	0	0.0	0.0
DIOS	1.77	0	0.0	0.0
FELIX	2.68	3	13.3	4.3
GLOR	3.19	1	14.0	4.9
GRUMO	3.22	3	17.0	4.2
GUAN	4.37	20	12.7	4.4
GUI	1.8	1	9.0	4.3
IND	1.82	1	34.0	4.5
MAND	1.84	0	0.0	0.0
MARIA	1.88	4	25.5	4.3
NDD	1.77	0	0.0	0.0
PACORA	1.84	1	94.0	4.1
PAN02	1.93	1	64.0	4.0
PAN06	2.5	0	0.0	0.0
PERE	1.84	0	0.0	0.0
PHW	1.79	0	0.0	0.0
PLA	1.79	0	0.0	0.0
PLS	1.83	1	35.0	4.1
PSM	1.79	0	0.0	0.0
ROBO	3.31	9	6.3	4.4
SAJ	1.83	0	0.0	0.0
SAN_T	1.82	0	0.0	0.0
SANPAB	2.1	1	98.0	4.5
SMP	1.78	0	0.0	0.0
TABA	2.44	4	37.0	4.6
VIGUI	2.31	1	101.0	4.1

SAMPLE ID	SeismicEvts10km	AvgDepth10km (km)	AvgMag10km (Mw)	SeismicEvts25m
ANT	0	0.0	0.0	4
BART	421	12.6	3.7	923
BLA	0	0.0	0.0	7
C_NATA	2	33.5	4.6	6
CAIM	1	13.0	5.3	5
CAPI	0	0.0	0.0	2
CHAG2009	4	57.5	4.7	12
CHAME	0	0.0	0.0	4
CHAN	152	18.2	3.7	408
CHVIE_H	21	22.8	4.0	117
CNGO	5	39.8	3.9	16
COBRE	4	75.0	4.3	13
CORO	289	13.1	4.0	810
CUAN	4	42.3	3.7	16
CUL	4	37.5	3.8	19
DIOS	1	30.0	4.0	7
FELIX	8	13.1	4.4	27
GLOR	15	7.3	4.1	65
GRUMO	45	18.4	4.1	132
GUAN	276	14.3	4.1	793
GUI	1	9.0	4.3	4
IND	3	261.3	4.4	7
MAND	7	39.6	3.4	18
MARIA	7	37.7	4.4	16
NDD	1	30.0	4.0	7
PACORA	4	62.3	4.2	8
PAN02	3	55.3	2.7	18
PAN06	3	29.7	4.5	10
PERE	0	0.0	0.0	2
PHW	1	75.0	6.2	10
PLA	2	52.5	5.1	11
PLS	6	54.7	3.8	12
PSM	1	75.0	6.2	11
ROBO	28	14.2	3.9	92
SAJ	0	0.0	0.0	2
SAN_T	4	62.3	4.2	5
SANPAB	3	76.7		8
SMP	1	30.0	4.0	9
TABA	11	27.9	4.4	20
VIGUI	3	67.3	4.3	15

SAMPLE ID	AvgDepth25km (km)	AvgMag25km (Mw)	SeismicEvts50km	AvgDepth50km (km)
ANT	35.8	4.3	12	82.8
BART	13.4	3.8	1489	15.0
BLA	47.6	3.3	27	35.7
C_NATA	27.8	4.4	16	26.4
CAIM	156.5	3.8	15	75.6
CAPI	23.5	4.9	9	100.2
CHAG2009	44.6	3.7	32	38.8
CHAME	35.8	4.3	14	74.6
CHAN	19.4	3.9	850	18.8
CHVIE_H	18.6	3.7	682	18.4
CNGO	39.1	3.6	36	36.2
COBRE	37.1	4.5	41	36.5
CORO	13.6	3.8	1442	14.8
CUAN	39.1	3.6	36	36.2
CUL	41.7	3.5	34	38.8
DIOS	47.6	3.3	31	36.9
FELIX	20.5	4.2	117	30.0
GLOR	16.0	4.0	228	20.7
GRUMO	19.0	3.9	328	20.2
GUAN	13.5	3.8	1441	14.7
GUI	35.8	4.3	13	76.9
IND	132.0	4.2	20	73.4
MAND	42.6	3.5	37	40.8
MARIA	34.4	4.4	43	29.7
NDD	47.6	3.3	31	36.9
PACORA	54.1	3.9	35	36.3
PAN02	40.8	3.2	39	40.7
PAN06	44.9	4.4	27	43.1
PERE	23.5	4.9	10	91.1
PHW	42.6	3.6	29	38.8
PLA	42.0	3.3	31	38.2
PLS	44.6	3.7	33	38.6
PSM	42.0	3.3	31	38.2
ROBO	17.7	4.0	338	19.6
SAJ	23.5	4.9	10	91.1
SAN_T	64.8	9.3	21	39.5
SANPAB	43.5	3.9	37	35.4
SMP	47.9	3.0	28	37.7
TABA	43.2	4.5	79	29.7
VIGUI	54.3	4.5	49	35.5

SAMPLE ID	AvgMag50km (Mw)	SeismicEvts75km	AvgDepth75km (km)	AvgMag75km (Mw)
ANT	4.5	31	46.5	4.1
BART	3.9	1891	15.6	4.0
BLA	3.4	55	45.9	3.9
C_NATA	4.5	42	30.0	4.3
CAIM	4.3	35	55.4	4.4
CAPI	4.0	23	56.0	4.2
CHAG2009	3.5	58	37.0	3.8
CHAME	3.8	25	52.1	4.1
CHAN	4.0	1620	17.0	3.9
CHVIE_H	3.9	1542	16.7	3.8
CNGO	3.5	65	35.6	4.0
COBRE	4.4	109	29.6	4.1
CORO	3.9	1835	15.5	4.0
CUAN	3.5	65	35.6	4.0
CUL	3.6	58	36.8	3.9
DIOS	3.4	54	34.2	3.9
FELIX	4.2	328	23.2	4.1
GLOR	3.9	696	17.7	4.0
GRUMO	4.0	1059	16.9	3.9
GUAN	3.9	1821	15.5	4.0
GUI	4.1	24	51.4	4.1
IND	4.3	32	53.0	4.3
MAND	3.7	68	37.3	3.9
MARIA	4.4	108	25.6	4.2
NDD	3.4	54	34.2	3.9
PACORA	3.5	59	35.4	3.9
PAN02	3.8	71	38.3	3.9
PAN06	4.6	65	48.8	4.2
PERE	3.6	25	56.9	4.3
PHW	3.5	54	34.2	3.9
PLA	3.4	60	43.9	4.0
PLS	3.6	59	36.6	3.8
PSM	3.4	60	43.9	4.0
ROBO	3.9	919	18.1	4.0
SAJ	3.6	17	65.1	4.0
SAN_T	3.2	53	36.4	3.8
SANPAB	4.4	101	29.3	4.1
SMP	3.5	54	34.2	3.9
TABA	4.2	215	25.5	4.1
VIGUI	4.4	134	27.3	4.1

SAMPLE ID	SeismicEvts100km	AvgDepth100km (km)	AvgMag100km (Mw)
ANT	46	53.1	4.3
BART	2121	16.0	3.9
BLA	81	45.0	4.0
C_NATA	91	34.4	4.2
CAIM	62	44.8	3.9
CAPI	41	52.4	4.3
CHAG2009	87	43.9	4.0
CHAME	48	52.5	4.2
CHAN	2072	17.1	3.9
CHVIE_H	2017	16.7	3.9
CNGO	90	43.6	4.1
COBRE	268	25.6	4.1
CORO	2106	15.8	3.9
CUAN	90	43.6	4.1
CUL	89	44.5	4.1
DIOS	79	42.9	4.1
FELIX	825	19.0	4.0
GLOR	1529	17.1	3.9
GRUMO	1882	17.3	3.9
GUAN	2110	15.7	3.9
GUI	40	57.0	4.3
IND	62	42.6	4.1
MAND	90	45.2	4.1
MARIA	212	27.4	4.2
NDD	79	42.9	4.1
PACORA	91	45.8	4.1
PAN02	89	39.2	4.1
PAN06	111	39.5	4.2
PERE	47	48.8	4.1
PHW	80	43.0	4.0
PLA	83	42.7	4.0
PLS	87	43.9	4.0
PSM	81	42.9	4.0
ROBO	1751	17.2	3.9
SAJ	43	55.7	4.3
SAN_T	80	44.3	4.0
SANPAB	235	25.0	4.1
SMP	79	43.1	4.0
TABA	534	21.7	4.0
VIGUI	332	24.1	4.1